INFORMATION TO USERS

This manuscript has been reproduced from the microfilm master. UMI films the text directly from the original or copy submitted. Thus, some thesis and dissertation copies are in typewriter face, while others may be from any type of computer printer.

The quality of this reproduction is dependent upon the quality of the copy submitted. Broken or indistinct print, colored or poor quality illustrations and photographs, print bleedthrough, substandard margins, and improper alignment can adversely affect reproduction.

In the unlikely event that the author did not send UMI a complete manuscript and there are missing pages, these will be noted. Also, if unauthorized copyright material had to be removed, a note will indicate the deletion.

Oversize materials (e.g., maps, drawings, charts) are reproduced by sectioning the original, beginning at the upper left-hand corner and continuing from left to right in equal sections with small overlaps. Each original is also photographed in one exposure and is included in reduced form at the back of the book.

Photographs included in the original manuscript have been reproduced xerographically in this copy. Higher quality 6" x 9" black and white photographic prints are available for any photographs or illustrations appearing in this copy for an additional charge. Contact UMI directly to order.

UMI®

Bell & Howell Information and Learning
300 North Zeeb Road, Ann Arbor, MI 48106-1346 USA
800-521-0600

Characterization of the *Meta*-Cleavage Pathway Enzymes, 4-Hydroxy-2-Ketovalerate Aldolase and Aldehyde Dehydrogenase (Acylating), from *Pseudomonas sp.* Strain CF600

Stavroula Monastiriakos

A Thesis

in

The Department

of

Chemistry

Presented in Partial Fulfillment of the Requirements
for the Degree of Magisteriate of Science at
Concordia University
Montreal, Quebec, Canada

July 1998

Abstract

Characterization of the *meta*-cleavage pathway enzymes, 4-hydroxy-2-ketovalerate aldolase and aldehyde dehydrogenase (acylating), from *Pseudomonas sp.* strain CF600

Stavroula K. Monastiriakos

Pseudomonas sp. strain CF600 is an efficient degrader of phenol and methylphenols. These toxic compounds are degraded by a set of enzymes encoded by the plasmid-located *dmp* operon. Ring cleavage and further metabolism follow initial hydroxylation of phenol to catechol via the *meta*-cleavage pathway. The final two steps of the *meta*-cleavage pathway involve the conversion of 4-hydroxy-2-ketovalerate to pyruvate and acetaldehyde, followed by oxidative acylation of acetaldehyde to acetyl-coenzyme A (Shingler, Powlowski & Marklund, 1992).

These final two reactions are catalyzed by the enzymes 4-hydroxy-2-ketovalerate aldolase and aldehyde dehydrogenase (acylating), encoded by *dmpG* and *dmpF*, respectively (Shingler, Powlowski, & Marklund, 1992). Both of the polypeptides, DmpG and DmpF, co-purify to homogeneity, indicating a tight physical association between them (Powlowski, Sahlman, & Shingler, 1993). It has been postulated that the close physical association between the two enzymes may allow the toxic acetaldehyde formed by the action of the aldolase to be channeled to the dehydrogenase.

The work presented in this thesis focuses on three aspects of the aldolase-dehydrogenase. First, DmpG was overexpressed and purified in order to address the question of whether this polypeptide alone possesses 4-hydroxy-2-ketovalerate aldolase activity. While previous work had indicated that DmpF alone can catalyze dehydrogenase activity, thus far no aldolase activity has been detected in preparations of DmpG. Second, steady-state kinetics studies of the individual and coupled reactions were performed in order to address the question of coupling. The data obtained are consistent with channeling of the aldolase product, acetaldehyde, to the dehydrogenase active site. Furthermore, kinetics measurements indicate either a partially or fully ordered terreactant mechanism for the dehydrogenase. Finally, chemical modification of the enzyme by iodoacetate provided evidence for the involvement of a reactive cysteine residue in dehydrogenase, but not aldolase, activity. This result is consistent with postulated mechanisms of other aldehyde dehydrogenases, and will allow creation of a variant that can be used to study the reactions of the aldolase separately from the dehydrogenase partner.

Acknowledgments

I would first and foremost like to thank my supervisor, Dr. Justin Powlowski, who for the past two years has guided me every step of the way. I would especially like to thank him for his relentless efforts in helping me shape this work into a thesis!

I would also like to thank my committee members, Dr. Muriel Herrington, and Dr. Joanne Turnbull. A special thanks to Dr. Turnbull for helping me decipher Fromm's version of enzyme kinetics.

I would also like to thank my fellow lab co-workers; Masoud, for showing me how to use Clustal, Nathalie, who showed me how to use Isis Draw, and Liz, for showing me where everything was when I came into the lab. I really enjoyed working with all of you.

A special thanks goes out to my friends and relatives especially Dinesh, Emma, Photini, and my cousin Niki, who has had to deal with my eccentricities!

I am also very grateful that I have wonderful parents, who sacrificed everything to turn me into the person that I am today. I hope you are as proud of me as I am of you.

....and of course, I would also like to thank my wonderful husband, Giovanni, who has been very supportive of me, and has helped me through a lot.....

Dedication

For my adored brother Peter,

There is not a moment that passes which doesn't reflect your laughing eyes, your beautiful smile, and your echoing laughter.

Αιωνια η μνημη

Table of Contents

Results

List of Figures

List of Tables

List of Abbreviations

Acet., Acetaldehyde

ALDH, Aldehyde Dehydrogenase

C18, Octadecyl

CoA, Coenzyme A

DTT, Dithiothreitol

EDTA, Ethylenediaminetetraacetate

HEPES, N-2-Hydroxyethyl Piperazine-N'-2-Ethanesulfonic Acid

IPTG, Isopropyl-1-Thio-β-D-Galactopyranoside

LDH, Lactate Dehydrogenase

MES, 2-[N-Morpholino]Ethanesulfonic Acid

mL, Milliliter

MOPS, 3-(N-Morpholino) Propanesulfonic Acid

NAD^+, Nicotinamide Adenine Dinucleotide

NADH, Reduced Nicotinamide Adenine Dinucleotide

PAGE, Polyacrylamide Gel Electrophoresis

PCR, Polymerase Chain Reaction

RP-HPLC, Reversed-Phase High Performance Liquid Chromatography

SDS, Sodium Dodecyl Sulfate

Tris, Tris[hydroxymethyl]aminomethane

Introduction

Introduction

Aromatic compounds demonstrate exceptional stability due to their cyclic conjugated π systems (Miller, 1992) and are thus relatively inert in biochemical systems. Consequently, when released into the environment some of these compounds become a nuisance, due to their persistence and toxicity. Numerous species of microorganisms have developed the ability to degrade naturally occurring aromatics for their metabolic needs. However when presented with man-made compounds, these organisms may fail due to the presence of structural features (eg. chlorination) that are not common in natural products. Therefore the study of existing degradative pathways is important in understanding the capabilities and limitations of these organisms. With enough knowledge of the genes and enzymes involved, strains may be constructed with improved metabolic efficiency, or with expanded substrate specificity for the catabolism of various environmentally significant compounds. (Timmis et al, 1994).

Phenol is a simple aromatic compound that is relatively biodegradable. It was first used as a disinfectant in 1867, by the British surgeon Joseph Lister, for sterilizing wounds, surgical dressings, and instruments (Microsoft ® Encarta ®, 1997). Dilute phenol solutions are useful as antiseptics, but concentrated solutions are caustic and can cause tissue scarring. Although phenol may have saved many lives by introducing the use of sterile technique, its general unhealthy effects on humans led to development of less toxic and more efficient germicides as replacements (Microsoft ® Encarta ®, 1997). Nevertheless, it is still used as a general disinfectant, and is used widely in the

manufacture of resins, plastics, insecticides, explosives, dyes, detergents, and as a raw material for the production of medicinal drugs such as aspirin, and acne medication (Microsoft ® Encarta ®, 1997). Therefore, it is produced in large quantities; in the United States alone, almost 1700 million kilograms are synthesized annually (Anonymous, 1993). In addition, huge quantities of substituted phenols are also produced industrially.

Microbial Catabolism of Phenol and Its Derivatives

The ability of some microorganisms to degrade phenol suggests that it may also be a naturally occurring compound. Indeed, phenol is produced by enterobacteria as a metabolic product of tyrosine, and from the breakdown of plant materials (Kumagai et al. 1970; Spoelstra, 1977). While much of our present knowledge of phenol degradation comes from investigations of various *Pseudomonas* species, other bacterial genera, such as *Bacillus*, as well as some species of yeast are also phenol degraders (reviewed by Powlowski & Shingler, 1994).

Degradation of phenol is initiated by its conversion to catechol (1,2-dihydroxybenzene). This initial oxygenation reaction renders the aromatic ring more susceptible to further attack by dioxygenases responsible for ring fission. Catechol also arises from the action of specific oxygenases on benzoic acid, anthranilic acid, naphthalene, salicylate, and other compounds (Dagley & Gibson, 1965; Assinder & Williams, 1990). Substituted catechols are formed in the catabolic pathways for methylated and chlorinated derivatives of the aforementioned compounds (Shingler et al, 1992).

While a diverse array of oxygenases convert aromatic compounds to catechol, the subsequent reactions of oxygenative ring fission and conversion to mainstream metabolites undergoes only one of two metabolic alternatives: an *ortho-* or *meta-* cleavage pathway for catechol (Figure 1). The pathway followed depends upon the nature of the microbial species and/or the nature of the growth substrate, as will be discussed below.

Chromosomally encoded enzymes catalyze the *ortho-* cleavage pathway for catechol in some species of bacteria. Cleavage of the catechol ring *between* the two hydroxyl groups is characteristic of this pathway (Figure 1): following ring cleavage a series of reactions yields β-ketoadipate, which is cleaved to the central metabolic intermediates, succinyl-CoA and acetyl-CoA (reviewed by Dagley, 1986). The *ortho-* cleavage pathway of pseudomonads cannot tolerate certain methyl-substituted substituents (Dagley, 1986). In some species, this is remedied by oxidizing the methyl group to a carboxyl, and then using a separate set of enzymes to degrade the resulting hydroxybenzoic acid (Dagley, 1986). Alternatively, methyl-substituted compounds that cannot be degraded by the *ortho-* cleavage pathway may be degraded by other species of bacteria, which possess plasmids encoding the methyl-tolerant *meta-* cleavage pathway.

The main distinguishing feature of the *meta-* cleavage pathway is that ring cleavage occurs *adjacent* to the two catechol hydroxyl groups (Figure 1). The subsequent series of reactions is dictated by the nature of the ring fission product, which is ultimately degraded to pyruvate, formic acid, and an aldehyde (Dagley & Gibson, 1965).

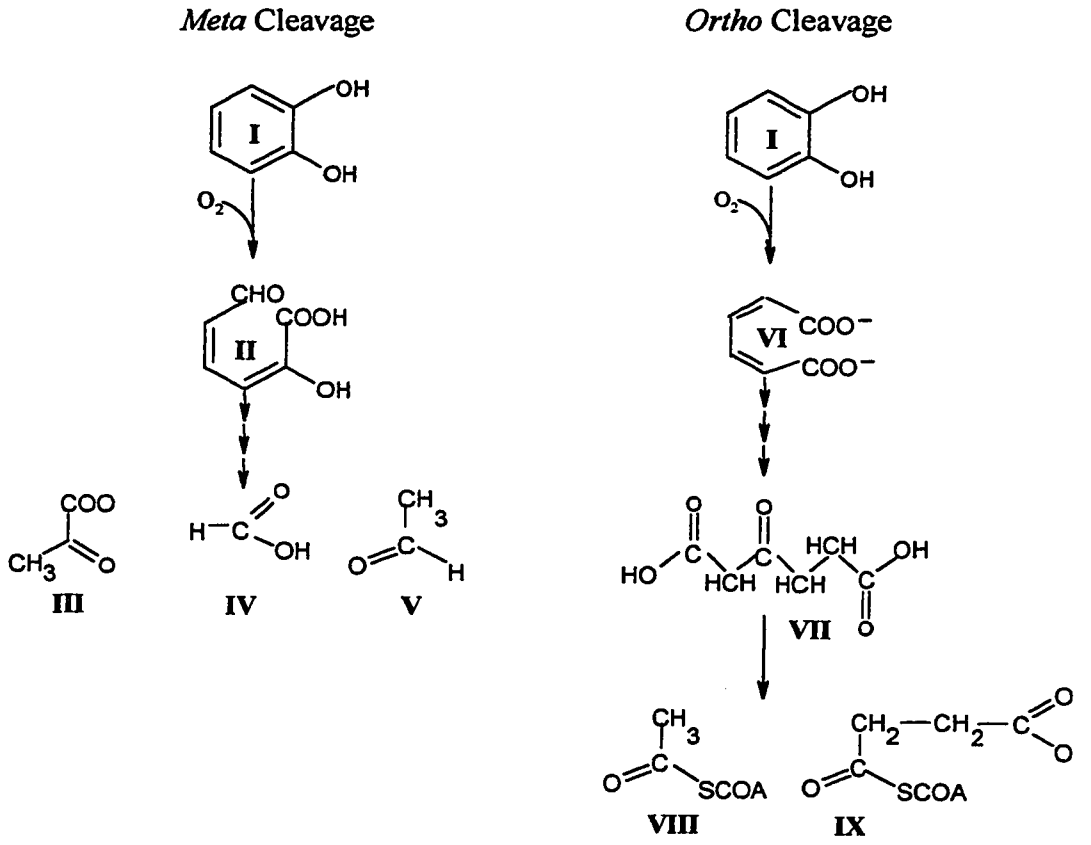

Figure 1: The two types of oxygenative ring fission of the catechol ring (compound I). The product of *meta* cleavage is initially II, 2-hydroymuconic semialdehyde, which is further converted to, III, pyruvate, IV, formate, and, V, a short chain aldehyde. The products of *ortho* cleavage is initially VI, *cis, cis*-muconate, which is converted first to VII, β-ketoadipate, and then to, VIII, succinyl-CoA, and IX, acetyl-CoA. Since the metabolic reactions that follow each type of ring cleavage are different, they constitute separate *meta* and *ortho* cleavage pathways.

The *Meta*-Cleavage Pathway in *Pseudomonas* sp. Strain CF600

The *meta*- cleavage pathway was first discovered in *Pseudomonas* strains that grow on phenols and cresols (Dagley & Gibson, 1965), and has subsequently been found in many different genera of bacteria, such as *Azotobacter,* and *Alcaligenes.* Even *Escherichia coli* K-12 metabolizes 3-phenylpropionic and 3-(3-hydroxyphenyl) propionic acids as sources of carbon via pathways that involve reactions of the lower part of the *meta*- cleavage pathway (Burlingame & Chapman, 1983). Although there is quite a bit of information on the pathway chemistry, gene organization, and regulation, work on the enzymology of the *meta*- cleavage pathway is far from complete.

Many features of the different *meta*- cleavage pathways are conserved among species of *Pseudomonas,* which grow at the expense of different aromatic compounds. *Pseudomonas putida* mt-2 bears an IncP-9 TOL plasmid, designated pWWO, which encodes a *meta*- cleavage operon induced by benzoic acid (Assinder & Williams, 1990). Benzoic acid is converted to catechol via benzoate oxygenase. *Pseudomonas putida* R1 harbours a plasmid in which the *meta*- cleavage pathway operon is induced by salicylate (Assinder & Williams, 1990). Here the initial enzymes of this pathway convert salicylate to catechol. Finally, the *meta*- cleavage operon of *Pseudomonas* sp. strain CF600 allows growth on phenol, cresols, and 3,4-dimethylphenol as sole carbon and energy sources (Shingler et al, 1989). The catabolic pathway for these substrates is encoded on pVI150, an IncP-2 megaplasmid exceeding 200 kb in size.

The fifteen structural genes encoding phenol degradation enzymes are clustered into a

single operon. The first six genes, *dmpKLMNOP*, encode a multicomponent phenol hydroxylase, which converts phenol to catechol. The remaining nine genes of the operon, *dmpQBCDEFGHI*, encode the *meta-* cleavage pathway, in which catechol is converted to pyruvate and acetyl-CoA (Figure 2). A brief description of the individual enzymes encoded by the *dmp* operon follows.

Initial Hydroxylation of Phenol

The first six genes of the *dmp* operon, *dmpKLMNOP*, encode a multicomponent phenol hydroxylase. However, only the gene products of *dmpLMNOP* (designated P1, P2, P3, P4, and, P5 respectively) are required for the *in vitro* activity of the hydroxylase (Powlowski & Shingler, 1994). It has recently been determined that DmpK represents a group of proteins, required by phenol degrading bacteria, for assembly of the active form of the oxygenase component of phenol hydroxylase (Powlowski et al, 1997).

Meta- Cleavage Pathway Enzymes

All of the *meta-* cleavage pathways use a common set of enzymes. The product of phenol hydroxylase, catechol (II), is cleaved and converted to 2-hydroxymuconic semialdehyde (III) by the gene product of *dmpB*, catechol 2,3-dioxygenase. This enzyme exhibits high sequence homology with other 2,3-dioxygenases from *meta-* cleavage pathways for other aromatic, extradiol ring fission compounds such as dihydroxylated naphthalene, and toluene (reviewed by Powlowski & Shingler, 1994). Its sequence similarity with other *meta-* cleavage dioxygenases, for example, those for 2,3 dihydroxybiphenyl, is much less (Furukawa et al, 1987).

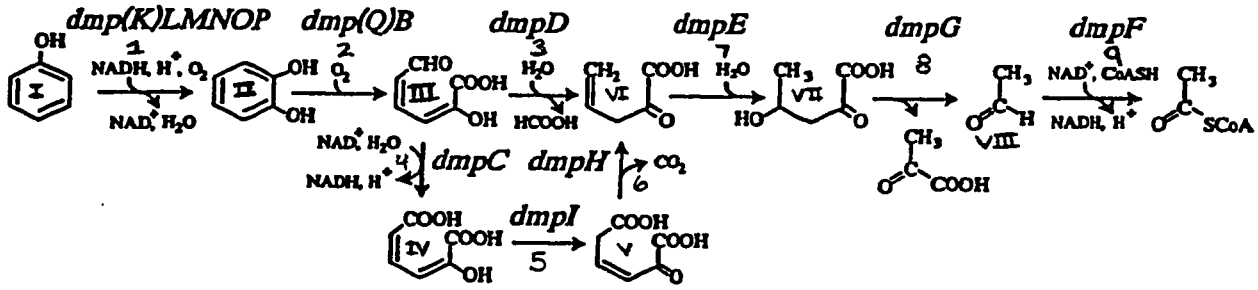

Figure 2: The pVI150 plasmid-encoded catabolic pathway for the degradation of phenol and its methylated derivatives. Compounds: I, phenol; II, catechol; III, 2-hydroxymuconic semialdehyde; IV, 4-oxalocrotonate, enol form; V, 4-oxalocrotonate, keto form; VI, 2-oxopent-4-enoate; VII, 4-hydroxy-2-ketovalerate, VIII, acetaldehyde. Enzymes: 1, phenol hydroxylase; 2, catechol 2,3-dioxygenase; 3, 2-hydroxymuconicsemialdehyde hydrolase; 4, 2-hydroxymuconicsemialdehyde dehydrogenase; 5, 4-oxalocrotonate isomerase; 6, 4-oxalocrotonate decarboxylase; 7, 2-oxopent-4-enoate hydratase; 8, 4-hydroxy-2-ketovalerate aldolase; 9, acetaldehyde dehydrogenase (acylating).

Figure taken from Powlowski & Shingler, (1994).

The *dmpQ* gene is located between genes coding for phenol hydroxylase and catechol 2,3- dioxygenase. DmpQ exhibits 41% sequence homology with plant type ferredoxins (Powlowski & Shingler, 1994). Expression of *dmpQ* is important for allowing strains to grow on 4-methylphenol, but not phenol, 2-methylphenol, or 3-methylphenol (Shingler & Powlowski, unpublished results). The presence of this ferredoxin-like protein could be to allow the bacterium to extend the substrate specificity of the *meta-* cleavage pathway, as does the homologous *xylT-* encoded ferredoxin (Harayama et al, 1993). Substrates channeled via 4-methylcatechol, which is a suicide substrate for catechol 2,3-dioxygenase, can therefore be metabolized.

DmpC and *dmpD* encoded enzymes both use the ring cleavage product (III) as a substrate and thus act as gatekeepers at the pathway branch (Figure 2). *DmpC* encodes 2-hydroxymuconic semialdehyde dehydrogenase (III), which converts 2-hydroxymuconic semialdehyde to 4-oxalocrotonate (enol form) (IV), reducing NAD^+ to NADH. The gene product of *dmpD*, 2-hydroxymuconic semialdehyde hydrolase, converts 2-hydroxymuconic semialdehyde (III) directly to 2-oxopent-4-enoate (VI). Hydrolase defective strains of *Pseudomonas putida* U failed to grow at the expense of phenols channeled through the pathway via 3-methylcatechol (Bayly & Wigmore, 1973). This is because the ring cleavage product yields a ketone (rather than an aldehyde), which cannot be oxidized by the dehydrogenase. The existence of this branch thus also helps to broaden the substrate specificity of the *meta-* cleavage pathway. Although the structures of the substrate are the same, DmpC and DmpD themselves do not share sequence homology, indicating different evolutionary origins (Powlowski & Shingler, 1994).

In the dehydrogenase-dependent branch of the pathway, the enzyme encoded by *dmpI*, 4-oxalocrotonate isomerase converts 4-oxalocrotonate (IV) from the enol form to the keto form (V). Studies using mutants of *Pseudomonas putida* U lacking this gene demonstrated that the enzyme is necessary to support growth on phenols channeled through catechol or 4-methylcatechol that are metabolized via this route (Wigmore et al, 1974). The enzyme encoded by *dmpH*, 4-oxalocrotonate decarboxylase, converts the keto form of 4-oxalocrotonate (V) to 2-oxopent-4-enoate (VI). It is at this point that the *meta*-cleavage pathway converges to enter the last three steps of the catabolic pathway.

The *dmpE* gene product, 2-oxopent-4-enoate hydratase, then converts 2-oxopent-4-enoate (VI) to 4-hydroxy-2-oxovalerate (VII). This enzyme has a close physical association with and co-purifies with the 4-oxalocrotonate decarboxylase (Powlowski et al, unpublished), as do the homologous *xyl*-encoded gene products (Harayama et al, 1989). Therefore, it has been proposed that the two enzymes are associated in order to channel the unstable intermediate that arise from the action of the decarboxylase (Harayama et al, 1989). However, no experimental evidence for this has been reported. Alternatively, there may be an evolutionary explanation for their close association. Sequence alignments indicate 37% identity between the sequences of *dmpH* and *dmpE*, which may indicate a common ancestry (Shingler, Powlowski, & Marklund, 1992). These enzymes could have evolved from a multimeric enzyme, which is why they are so tightly associated with each other. These are the only two enzymes in the pathway that appear to have arisen via gene duplication and divergence (Powlowski & Shingler, 1994).

Close physical association has also been demonstrated for the last two enzymes, DmpF and DmpG, of the *dmp*-encoded pathway. These proteins co-purify through five chromatographic steps, and an ammonium sulphate fractionation step (Powlowski, Sahlman, & Shingler, 1993). The complex (148 kDa) appears to be made up of two subunits each of DmpF (40 kDa) and DmpG (35 kDa) (Powlowski & Shingler, 1994). Unlike DmpE and DmpH, DmpF and DmpG do not share any sequence homology, indicating separate evolutionary origins (Powlowski & Shingler, 1994).

The *dmpG* gene product, 4-hydroxy-2-ketovalerate aldolase, converts L-4-hydroxy-2-ketovalerate (VII), produced by DmpE, to pyruvate and acetaldehyde (VIII). This metal dependent aldolase has been reported to be similar to other *meta*- cleavage pathway aldolases (Powlowski & Shingler, 1994). A Blast sequence homology search demonstrated that the *dmpG* nucleotide sequence shows high sequence homology to many other 4-hydroxy-2-ketovalerate aldolases, but not to other enzymes that catalyze aldol cleavage. It also shares sequence homology with several homocitrate synthases, and isopropylmalate synthases. Although the homologies with the synthases are not as high as with the 4-hydroxy-2-ketovalerate aldolases, these condensation reactions are mechanistically simply the reverse of the 4-hydroxy-2-ketovalerate aldolase-catalyzed reaction. Therefore it is not surprising that these enzymes appear to be related (Shingler, Powlowski, & Marklund, 1992).

Pyruvate is a central metabolic intermediate, and is produced, along with acetaldehyde, by the action of the aldolase. Acetaldehyde is a substrate for DmpF, which converts it to

acetyl-CoA with the concomitant reduction of NAD^+. It has been suggested that the tight association between the aldolase and the last enzyme in the pathway may be in order to channel the toxic aldehyde from the active site of the aldolase, (DmpG), directly to the dehydrogenase, (DmpF), consequently ensuring its efficient metabolism and minimizing its toxicity (Powlowski & Shingler, 1994).

What makes the aldehyde dehydrogenase so interesting is that metabolism of acetaldehyde in many other organisms involves oxidation of the acetaldehyde to acetate and then a subsequent ATP dependent reaction to acetyl-CoA (Hempel et al, 1993). The *dmpF*-encoded *meta-* cleavage pathway enzyme thus represents an energetically efficient form of aldehyde metabolism. This enzyme is also capable of acylating propionaldehyde (Powlowski, Sahlman, & Shingler, 1993) which would be formed by the catabolism of certain methylated phenolic derivatives (Dagley & Gibson, 1965). The sequence of this novel enzyme is very similar to several other acylating aldehyde dehydrogenases from *Pseudomonas putida* and *E. coli*, and less similar to aspartate-semialdehyde dehydrogenase, and glyceraldehyde 3-phosphate dehydrogenase. The enzymes that are homologous to DmpF have not been well characterized. The amino terminal of DmpF has been shown to encompass an NAD^+ binding site, which contains a characteristic ADP-binding fingerprint sequence (Powlowski & Shingler, 1994). Its shares no sequence homology with the other dehydrogenase in the pathway (HMSD, which catalyses step 4, Figure 2), which demonstrates that they have two different evolutionary origins (Powlowski & Shingler, 1994).

The work reported in this thesis carries on the characterization of the DmpG (4-hydroxy-2-ketovalerate aldolase) and DmpF (aldehyde dehydrogenase, acylating). It is therefore appropriate to briefly review the biochemistry of aldolases and aldehyde dehydrogenases.

Review of Aldolase Biochemistry

Aldolases catalyze a variety of condensation and cleavage reactions, with great control of the stereochemistry, especially in sugar metabolism. As a result these enzymes are potentially useful catalysts for synthetic chemistry. Aldolases can be generally classified into two classes: Class I which rely on a catalytic active site lysine residue; and Class II, which require a divalent metal ion, as is the case for 4-hydroxy-2-ketovalerate aldolase, DmpG.

Class I Aldolases

A type I aldolase is distinguished from its type II counterpart on the basis of its ability to catalyze aldol cleavage without involvement of a metal ion. The active site of a type I aldolase contains a Lys residue that forms a covalent Schiff base intermediate during the catalytic cycle (Horecker et al, 1972). Aldehydes and ketones react with primary amines to form imines; an N-substituted imine is designated a Schiff base.

Three type I aldolase structures have been determined; rabbit, human and *Drosophila melanogaster* enzymes have all been found to be structurally similar. All of these enzymes are tetramers with threefold axis symmetry (Littlechild & Watson, 1993). The

inter-subunit contacts are essentially the same in all three enzymes, and the subunits are composed of a β-barrel-type structure, which is surrounded by α-helices and connecting loops. Active site residues as well as those assumed to bind substrates are conserved.

Since the enzymes are structurally similar it has been proposed that they proceed via the same mechanism (Littlechild & Wason, 1993). Mechanistic data has only been collected for rabbit and human muscle aldolase. The best characterized type I aldolase thus far is the glycolytic enzyme which cleaves fructose 1,6-bisphosphate to form dihydroxyacetone phosphate and glyceraldehyde 3-phosphate. An enzymatic mechanism involving the active site lysine residue 146 has been elucidated (Littlechild & Watson, 1993).

Class II Aldolases

In contrast to the class I aldolases, in class II aldolases, a metal ion, rather than a Schiff base acts as an electron sink for the stabilization of the reaction intermediate and for the activation of the bound substrate. Amino acid sequence comparisons with class I aldolases show no homology (Dreyer et al, 1993). In general, most class II aldolases use a divalent cation to fulfill their metal requirements, but depending on the enzyme, the metal may vary; some aldolases utilize Zn^{+2} (Dreyer et al, 1993), some Mg^{+2}(Dagley & Gibson, 1965) or even Mn^{+2} (Powlowski, Sahlman & Shingler, 1993).

Two type II aldolase structures have been determined by X-ray crystallography. The first one, L-fuculose-1-phosphate aldolase, from *E.coli,* catalyses the reversible cleavage of L-

fuculose-1-phosphate to dihydroxyacetone phosphate and L-lactaldehyde in bacterial fuculose metabolism. It shows no obvious similarity to the known structures of class I aldolases, except that it is also a homotetramer. It exhibits uncommon features for the overall chain fold, quaternary structure, and the co-ordination of the catalytically active zinc ion (Dreyer et al, 1993).

The chain fold of a single subunit of L-fuculose-1-phosphate aldolase is roughly ellipsoidal, and is built around a nine-stranded β-pleated sheet (Dreyer et al, 1993). The sheet is covered by two α-helices on one side and three on the other side. This chain fold is rather special because it is quite uncommon. The catalytic zinc ion is bound by four side-chains, His 92, His 94, His 155 and Glu 73, but in the shape of a distorted co-ordination sphere. The pattern of long and short sequences between the zinc ion ligands seems to be characteristic, and it has been found in other Zn^{+2} containing enzymes also (Vallee & Auld, 1992). What is apparently unusual is that all other presently known catalytic zinc sites provide only three residues for co-ordination while the fourth coordination site is occupied by water.

A similar metal-binding motif is not observed in the 4-hydroxy-2-ketovalerate aldolase. Although the enzyme contains nine histidines, they are not arranged in a similar pattern. A glutamate residue is altogether missing from this particular aldolase.

The crystal structure of a class II fructose-1-6-bisphosphate aldolase has also been recently determined (Cooper et al, 1996). In this case the enzyme is dimeric, and

comprises an $(\alpha/\beta)_8$ barrel tertiary structure. On the basis of structure alone, the researchers suggest that this particular enzyme shares the same mechanism as the other type II fuculose aldolase. A novel structural feature of this enzyme is that the active site contains a bimetallic binding site with two metal ions. One ion whose identity was not elucidated remains buried, and may play a structural or activating role in catalysis, while a catalytic zinc is positioned at the surface of the barrel. Sequence homology with other type II aldolases, such as L-fuculose-1-phosphate aldolase, reveals that this enzyme may share common ancestry with them, even though it features a different subunit size, fold, quaternary structure, and different metal ion-binding sites (Cooper et al, 1996).

With these new differences coming to light between the class II aldolases it has been suggested that class II aldolases should be subdivided into two categories based on consideration of the aforementioned differences. A Blast sequence homology search yielded no significant similarity between either of the type II enzymes described above and 4-hydroxy-2-ketovalerate aldolase.

Review of Aldehyde Dehydrogenase Biochemistry

While CoA-linked aldehyde dehydrogenases like DmpF have not been studied in great detail, much is known about non CoA-linked aldehyde dehydrogenases. Some of this information appears to be relevant to the CoA-linked variants, which justifies a brief review of the properties of aldehyde dehydrogenases.

Aldehyde dehydrogenase is famous for its conversion of ethanol derived acetaldehyde to acetate, and for its conversion of amine derived aldehydes to their corresponding carboxylic acids. High levels of aldehydes in cells are deleterious, leading to cytotoxicity, mutagenicity and carcinogenicity (Lindahl & Hempel, 1990). By converting aldehydes to their corresponding carboxylic acids, aldehyde dehydrogenases render them less reactive.

Aldehyde dehydrogenases occur with wide phylogenic distribution. The variety of organisms they have been found in ranges from mammals to bacteria, fungi, and higher plants (Lindahl & Hempel, 1990). These enzymes exist in multiple molecular forms, which differ in their physical and/or their functional properties. Tetrameric and dimeric functional forms have been discovered. Some forms have been found which display broad substrate specificity, oxidizing an array of aliphatic and aromatic aldehydes. Others are much more stringent, preferring some substrates to others (Hempel et al, 1993). While all aldehyde dehydrogenases most likely use NAD^+ as a coenzyme *in vivo*, certain forms also utilize $NADP^+$ in vitro (Hempel et al, 1993). Various alignments of ALDH sequences have revealed 32-95% amino acid sequence identity (Lindahl & Hempel, 1990).

The sequences of aldehyde dehydrogenases share a relatively common core, with an almost even balance of polar, nonpolar, and charged residues: exceptions are some enzymes from *Pseudomonas*, and rat liver microsomal enzyme (Hempel et al, 1993).

Other similarities include conservation of hydrophobic, basic, and acidic residues which are probably important for interior-packing interactions.

The nucleotide-binding domain of aldehyde dehydrogenases has been localized to the amino-terminal half of the protein. The consensus sequence for this binding motif is GXGXXG, which reflects the turn at the end of the first β-strand in the first mononucleotide-binding unit of the Rossmann fold, which interacts with the adenine ribose of NAD^+ (Hempel et al, 1993). This motif is also found in the N terminal region of DmpF, where the actual sequence is GSGNIG between residues 11-16. For ALDH the structure shows that each subunit of the dimeric enzyme contains an NAD^+ binding domain, a catalytic domain, and a bridging domain. At the interface of the two domains is a funnel shaped pocket, which leads to a catalytic pocket (Zhie et al, 1997).

In mammalian ALDHs, an invariant cysteine residue has been generally regarded as the catalytic cysteine (Hempel et al, 1993). Many papers have confirmed the role of the cysteine residue for aldehyde dehydrogenases through site-directed mutagenesis (e.g. Gilberger et al, 1997). Aldehyde dehydrogenases are thought to function by forming a covalent S-acyl enzyme intermediate via the catalytic cysteine as is shown in Figure 3.

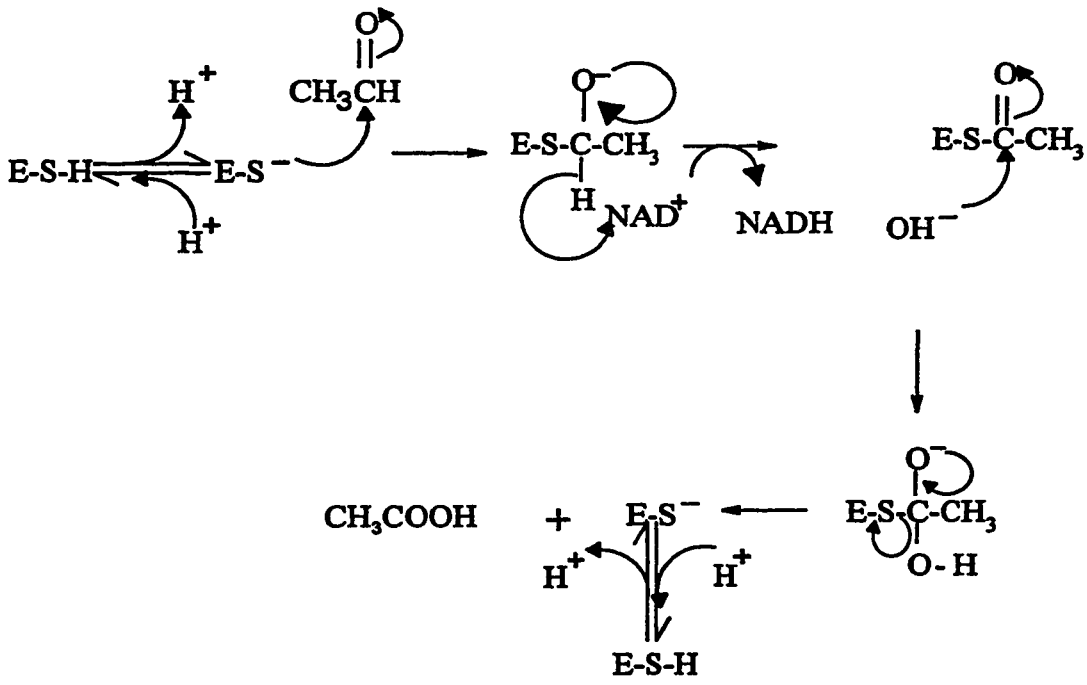

Figure 3: The postulated role of the catalytic cysteine residue in aldehyde dehydrogenase. Formation of an S-acyl intermediate is postulated. In an acylating dehydrogenase like DmpF, replacement of OH^- by $CoAS^-$ would lead to the formation of the observed thioester product. The enzyme with the active site thiol is designated E-S-H.

Coenzyme A-linked Aldehyde Dehydrogenases

Unfortunately, there is relatively little literature currently compiled on coenzyme A-linked aldehyde dehydrogenases. Aside from basic biochemical characterization, reported work concentrates on the kinetic mechanisms of these enzymes. In three substrate, two-product systems such as these, several kinetic mechanisms are possible (Cleland, 1963). One possibility is the ter bi mechanism in which all three substrates bind to the enzyme to form a quaternary complex followed by release of both products. Alternatively, in a bi uni uni uni ping-pong mechanism, two substrates bind, a product is released, the last substrate binds, and then the final product is released. Finally, a uni uni bi uni ping- pong mechanism occurs when a substrate binds, a product is given off, then two substrates bind and then the final product is released. In all three cases these mechanisms could be either random, ordered or mixed type systems (Segel, 1975).

The best-characterized CoA-linked aldehyde dehydrogenase thus far appears to be that from *Clostridium kluyveri.* This organism is unique, since it can grow on an extremely simple medium that consists only of ethanol and acetate as sole sources of carbon and energy (Smith & Kaplan, 1980). The only known reaction in the fermentation pathway of this bacterium, catalyzed by a coenzyme A-linked aldehyde dehydrogenase, is where acetaldehyde is converted to acetyl coenzyme A in an NAD^+ -dependent reaction.

The *C. kluyveri* enzyme was purified to about 40% homogeneity. It has a molecular weight of 290 000 kDa, in the presence of substrate. The aldehyde dehydrogenase was able to utilize thiols other than CoA, such as pantetheine, 2-mercaptoethanol, dithioerythritol, glutathione and cysteamine. Broad thiol specificities have also been found in pig heart and sheep liver dehydrogenases (Rudolph et al, 1968).

Initial velocity, product inhibition, and substrate inhibition measurements (Smith & Kaplan, 1980) examined physical and kinetic properties of the *C. kluyveri* enzyme. The double reciprocal plots and replots with the three varied substrates were consistent with a ping-pong mechanism for the *C. kluyveri* CoA-linked aldehyde dehydrogenase: in this mechanism, the binding of substrates is interrupted by the release of products. Unlike CoA independent aldehyde dehydrogenases, the *C. kluyveri* enzyme undergoes a bi uni uni uni ping-pong mechanism. In the proposed kinetic mechanism, shown in Figure 4, NAD^+ binds to free enzyme, followed by acetaldehyde, NADH is released and CoA binds after its release, and finally acetyl coenzyme A is formed.

Substrate inhibition by CoA was also observed for the CoA-linked dehydrogenase from *C. kluyveri*. The authors postulate that the observed inhibition may give insight into the coenzyme binding sites on the enzyme; inhibition may occur because both coenzymes share a common adenosine-binding site. Alternatively, they may have distinct binding sites but CoA is recognized as a nucleotide by the NAD^+ binding site (Smith & Kaplan, 1980). NAD^+ did not appear to inhibit the binding of CoA, perhaps because the bulky nicotinamide mononucleotide prohibits binding at this site (Smith & Kaplan, 1980).

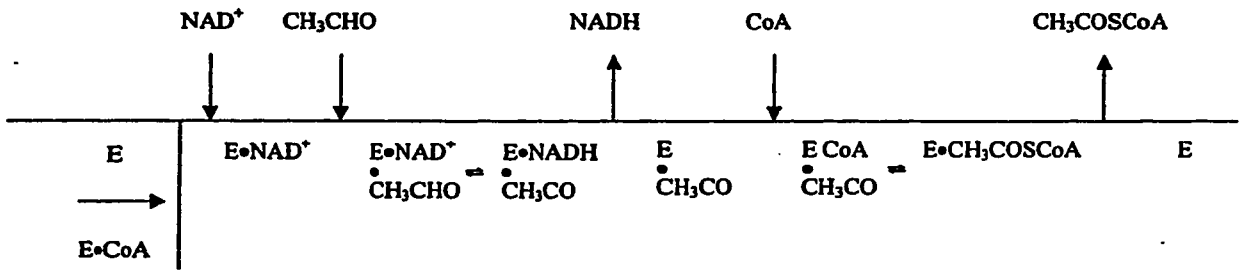

Figure 4: The proposed ping-pong kinetic mechanism of *C. kluyveri* CoA linked aldehyde dehydrogenase (Smith & Kaplan, 1980). NAD^+ binds to free enzyme before acetaldehyde, acetaldehyde binds, NADH is released, CoA binds last, and finally acetyl –CoA is released. The E•CoA complex shown at the beginning depicts the form involved in the inhibition observed by the CoA.

The figure was reproduced from the original in Smith & Kaplan, (1980).

A CoA-linked aldehyde dehydrogenase from *Escherichia coli* has also been partially purified and characterized. For this enzyme, a ping-pong mechanism has also been found (Rudolph, Purich, & Fromm, 1968), but this seems to be the only similarity with the *Clostridium kluyveri* enzyme. Substrate inhibition by CoA was not observed with the *E. coli* enzyme.

Metabolite Channeling

The direct transfer of a metabolite from the active site of one enzyme to the active site of another enzyme in a sequential pair is referred to as substrate channeling. This possibility has previously been raised to explain why DmpF and DmpG are physically associated (Powlowski et al, 1993). Channeling ensures enzymatic efficiency by transferring the product of the first enzyme into the active site of the second enzyme, without release into bulk solution. This may be important in the case of unstable or toxic intermediates. Whether channeling occurs is often a controversial issue; especially when the enzymes involved in the channel do not form a stable complex that can be isolated (Cornish-Bowden, 1995). With the aid of crystallographic work, it has become possible to visualize how the transfer of metabolites occurs in some enzymes. The best-

characterized and least controversial example of substrate channeling in a multienzyme complex comes from studies done with tryptophan synthase.

Tryptophan synthase is an enteric bacterial enzyme, with a subunit composition of $\alpha_2\beta_2$. The enzyme catalyzes the last two steps in the synthesis of L-tryptophan, consecutive processes that depend on the channeling of the intermediate, indole, between the active sites of the α and β subunits through a 25 Å-long tunnel. The α subunit has an $(\alpha/\beta)_8$ barrel folded motif and catalyses the cleavage of 3-indole-D glycerol 3-phosphate to indole and D-glyceraldehyde-3-phosphate. The β subunit is a pyridoxal phosphate requiring enzyme that catalyses the conversion of L-serine and indole to L-tryptophan and a water molecule (reviewed by Pan et al, 1997).

The reactions involved occur in two stages, as illustrated in Figure 5. In stage I, L-serine reacts with enzyme bound pyridoxal 5' phosphate to form a quasi stable intermediate, α-aminoacrylate, E(A-A), the species which reacts with the indole. In stage II indole reacts with E(A-A) to form L-tryptophan. The coupling of the activities of the two active sites are controlled by allosteric signals derived from covalent transformations at the β-site,

which convert the whole enzyme from a low (open, substrates bind and products are released) to a high (closed for cleavage of IGP) activity state (Pan et al, 1997).

In order for there to be efficient channeling occurring between enzyme pairs, there are many physical and dynamic constraints that must be satisfied (Pan et al, 1997). Primarily, the architecture of the complex must be so that direct transfer of the metabolite is ensured. An interconnecting tunnel is insufficient to ensure channeling and has been observed (Pan et al, 1997). In the case of the indole formed by the tryptophan synthase it must also be prevented from escaping the bienzyme complex (Pan et al, 1997). Aside from that, catalysis at the two active sites must be coupled in such a manner that the turnover at each individual site occurs in phase. In order to phase the reactions occurring at the α-site with those at the β-site, there is an allosteric signaling mechanism operating between the two catalytic sites, that switches catalysis on and off (Pan et al, 1997).

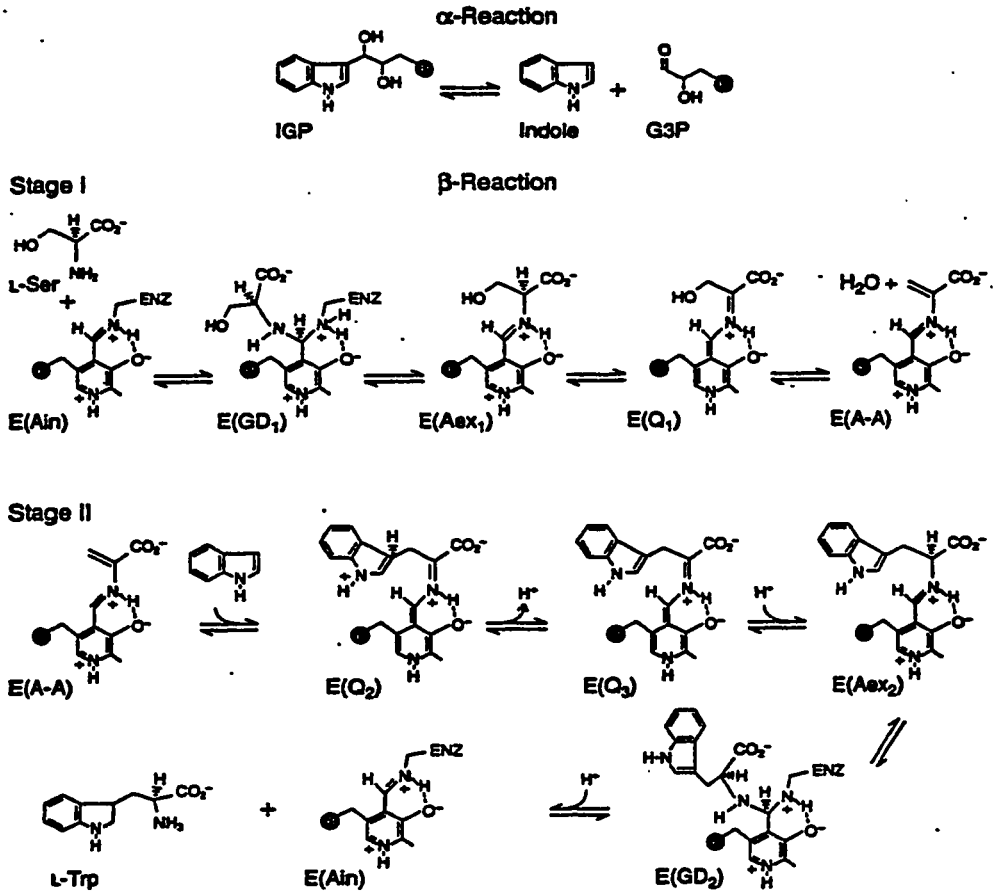

Figure 5: Reaction pathways for the tryptophan synthase bienzyme complex. The α-reaction cleaves 3-indole-D-glycerol 3'phosphate (IGP) to give indole and D-glyceraldehyde-3-phosphate (G3P). In stage I of the β-reaction, L-Ser is converted to a quasistable species, the α-aminoacrylate Schiff base, E (A-A); in Stage II, the indole produced in the α-reaction reacts with E (A-A) to yield L-Trp.

This figure is from Peng et al, (1997).

Along with the physical and dynamic constraints, kinetic evidence also exists for metabolite channeling in tryptophan synthase. The conversion of indole-3-glycerol phosphate to tryptophan at the active site proceeds at a rate of 24 s^{-1}, which is limited by the rate of cleavage of IGP to produce indole (α-reaction) (Anderson, et al, 1991). In a single turnover experiment monitoring the conversion of IGP to tryptophan, only trace amounts of indole was detectable, implying that the reaction of indole to form tryptophan must be quite fast (> 1000 s^{-1}) (Anderson, et al, 1991). The rate of reaction of exogenous indole from solution to tryptophan is too slow (at 40 s^{-1}) to account for the negligible accumulation of indole in a single turnover. Therefore, the indole produced at the α-site must be channeled to the β-site so that it can react rapidly with serine to form tryptophan.

Materials and Methods

Materials and Methods

Materials and Chemicals

All chemicals were reagent grade or higher.

Preparation and Quantitation of CoA, NAD^+ and NADH Solutions

The solutions used in the enzymatic assays were prepared as follows: CoA was dissolved in water (10 mg/mL), NAD^+ was dissolved in 50 mM Mes-NaOH, pH 6 (20 mg/mL), and NADH was dissolved in 50 mM HEPES, pH 8.0 (23 mg/mL). Concentrations were determined by adding 5µl of each stock solution to phosphate buffer (1 mL) at room temperature, and determining absorbance values at 260 nm for CoA and NAD^+, and at 340 nm for NADH. Extinction coefficients of 16800 $M^{-1}cm^{-1}$, 17800 $M^{-1}cm^{-1}$, and 6220 $M^{-1}cm^{-1}$, respectively, were used to determine concentrations of the stock solutions (Dawson et al, 1986).

Preparation and Purification of 4-hydroxy 2-ketovalerate

The L-(*S*) substrate for 4-hydroxy-2-ketovaletate aldolase was synthesized from L-(*S*)-4-methyl-2-ketobutyrolactone which was obtained as described previously (Burlingame & Chapman, 1983; Shingler, Powlowski & Sahlman, 1992). The starting lactone had previously been determined as being pure using C-18 reversed-phase HPLC (Powlowski, Sahlman, & Shingler, 1993).

As described previously (Dagley & Gibson, 1965), 4-methyl-2-oxobutyrolactone, (11.4

mg) was dissolved in distilled water (9.9 mLs) and (0.1 mL) of a 1N NaOH solution and was subjected to mild alkaline hydrolysis overnight at room temperature. Sixteen hours later, the hydrolysis mixture was loaded onto an octadecyl solid phase extraction cartridge (B&J Solid Phase system, Burdick and Jackson, 900 mg) previously washed with methanol (20 mL) and equilibrated with water (10 mL). 4-Hydroxy-2-ketovalerate did not bind to the column, so a 12 mL fraction was collected, a portion was quantified as described below, and 500 µL fractions were stored at –20 °C until further use.

HPLC Analysis

High-performance liquid chromatography of 4-hydroxy-2-ketovalerate formation was carried out using a BioRad HPLC chromatograph equipped with an OD5 Octadecyl reversed-phase column (Burdick and Jackson, Muskegon, Mich.). Detection was performed at 230 nm. After injection of sample, water was washed through the column (1 mL/min). The methanol concentration was increased to 30% over the next five minutes, followed by an increase to 100 % methanol over the next five minutes. Finally 100 % water was washed through for the last five minutes. The 4-hydroxy-2-ketovalerate had a retention time between 3.5 and 4.5 minutes.

Preparation of Acetaldehyde Stock Solutions

In order to quantitate the volatile substrate acetaldehyde, an enzymatic method using alcohol dehydrogenase was employed (Bernt & Bergmeyer, 1965). The assay (1mL) proceeded at room temperature and contained 50 mM Na^+K^+ phosphate, pH 7.5, NADH (100 µM), and diluted acetaldehyde (up to 50 µM). After recording the initial absorbance

reading at 340 nm, the reaction was initiated by the addition of alcohol dehydrogenase (150 U). The reaction was allowed to reach completion, and after 25 minutes the final absorbance reading was taken. The change in absorbance at 340 nm corresponds to the amount of NADH converted to NAD^+ by alcohol dehydrogenase, which in turn represents the amount of acetaldehyde present in the reaction cuvette.

Protein Purification

The purification of native DmpFG from phenol grown *Pseudomonas sp.* strain CF600 was accomplished using a previously published method (Powlowski et al, 1993). The purification of DmpG from *Pseudomonas putida* strain PB2701 was essentially using the same method, with the omission of the ammonium sulfate fractionation step. Specific activities for the native DmpFG preparation were 60 Units of 4-hydroxy-2-ketovalerate aldolase and 58 Units for aldehyde dehydrogenase (acylating) activity, comparable to the published values of 68 and 64 Units, respectively (Powlowski, Sahlman, & Shingler, 1993).

Cell Fractionation

Crude extracts of *E. coli* BL21 (DE3) harboring the expression plasmids were prepared by sonication using a Branson Sonifier 250. The cell paste was resuspended in sonication buffer (50 mM Na^+K^+ phosphate buffer pH 7.5 + 0.1M NaCl). Generally the volume used was 100X less than the volume of original growth media. Cells were sonicated using 7-second bursts at power level three, with intermediate cooling periods. The number of bursts varied with the volume of resuspended cells: generally, 50 grams of

cells in 40 mL of sonication buffer required about ten bursts at a setting of three. Cell debris was then removed by centrifugation at 4 °C for 45 minutes at 15,300 x g. Samples of the supernatant and pellet were subjected to protein assays, enzyme assays, and polyacrylamide gel electrophoresis.

Inclusion Body Purification

Depending on the expression conditions, DmpF and DmpG were often found in inclusion bodies. In order to be able to attempt purification from inclusion bodies the inclusion bodies were first purified and then solubilized in urea (Marston & Hartley, 1990). After cell breakage by sonication and separation of the insoluble fraction by centrifugation, the pellet was resuspended in 50 mM Na^+-K^+ Phosphate buffer, pH 7.5, containing lysozyme (0.2 mg/mL), EDTA (1 mM), and sodium deoxycholate (1 mg/mL). This suspension was incubated on ice for 20 minutes, and then centrifuged at 11,410 x g for 45 minutes. The supernatant was removed, and the pellet was resuspended in ice cold water, followed by centrifugation at 15,300 x g for 30 minutes. The supernatant was discarded and the pellet was then solubilized in 6 M urea. Once the pellet was dissolved, the sample was centrifuged at 15,300 x g for ten minutes to remove the remaining insoluble material, and the supernatant containing solubilized protein was either stored at -20 °C for later use or dialysed to remove the urea.

Dialysis tubing (Spectra/Por) was prepared as described (Sambrook, Fritsch, & Maniatis, 1989) and stored at 4 °C in 1 mM EDTA and 20% ethanol. Dialysis for urea removed was always performed in the cold over a minimum of 16 hours, and involved at least 4

buffer changes. Samples were removed from the dialysis bags, and centrifuged at 4 °C at 7,520 x g to remove any precipitate before further use.

Plasmid Constructs and Strains

Strains and plasmids used in this study are listed in Table 1. DNA manipulations were performed according to standard techniques (Sambrook, Fritsch & Maniatis, 1989). In order to construct plasmids for independent overexpression of DmpF and DmpG, *dmpF* and *dmpG* were first amplified using PCR designed to incorporate *BamH1* and *Nde1* restriction enzyme sites (shown in boldface). The primer sequences were: GGA GCT GCC **ATA TG**A CGT TCA ATC CG, and CGG GTC AGA GTG CGG TTC A**GG ATC** CG . The polymerase chain reaction was successful for *dmpG* amplification only when a concentration of 1.0 mM $MgCl_2$ was used for the reaction. The standard $MgCl_2$ concentration of 1.5 mM was used for *dmpF* amplification. The amplified product was cloned into the pCRII vector (Invitrogen). Both strands of the products were sequenced (Silver Stain Sequencing Kit, Promega) to ensure that mutations had not been introduced during amplification.

DmpF and *dmpG* were transferred on *Nde1* - *BamH1* fragments from pCRII into the T7-promoter based pET3a (Hanahan, 1985) and pSBET (Schenk et al, 1995) vectors for overexpression: this resulted in constructs, pET3a (*dmpF*), pET3a (*dmpG*), pSBET (*dmpF*) and pSBET (*dmpG*). Plasmids were purified using the Wizard Plus Minipreps DNA Purification System (Promega). Purifications of DNA fragments from agarose

Table 1: Bacterial strains and plasmids used in this study: References are shown in brackets.

Strain or Plasmid	Properties/Genes
Strains	
E. coli DH5	$r^- m^+$ *recA1* (Hanahan, 1985)
E. coli BL21 (DE3)	Protease $^-$ strain expressing T7 RNA polymerase under the control of the *tac* promoter (Rosenburg et al, 1987)
Pseudomonas sp. CF600	Phenol, 3,4-dimethyl phenol degrader (Shingler et al, 1989)
P. putida PB2701	$r^- m^+$ $Strep^R$ derivative of KT2440 (MBSC, M. Bagdassarian strain collection)
Plasmid	
pMMB66Δ	Amp^R RSF1010 based *tac* promoter expression vectors with *lacI* deletion (Shingler et al, 1989)
pVI310	*dmpF*, *SalI-SalI* fragment in pMMB66 (Shingler et al, 1992)
pVI312	*dmpG*, *SauI-BstEII* fragment in pMMB66 (Shingler et al, 1992)
pET3a	Amp^R T7 promoter expression vector (Hanahan, 1985)
pSBET	Kan^R T7 promoter expression vector (Schenk et al, 1995)
pCRII	Amp^R and Kan^R cloning and sequencing vector (Invitrogen)

gels were performed using the Sephaglas BandPrep Kit (Pharmacia Biotech).

Preparation of Competent Cells

Competent cells were prepared using a protocol cited in the literature supplied with the U.S.E. Mutagenesis kit (Pharmacia).

Electroporation Procedures

The procedure for preparing electrocompetent *Pseudomonas* cells was obtained from Professor Victoria Shingler (personal communication). *Pseudomonas* PB2701was grown at 30 °C in LB containing streptomycin (1000 μg/ml) until the OD_{650} was 0.7-0.9. The cells were harvested at 4 °C at 7,520 x g for ten minutes. The cell pellet was then resuspended in 1X culture volume of ice-cold sterile water, and harvested as in the previous step. The pellet was then washed in 1/2X culture volume ice-cold sterile water. The cells were resuspended in 1/10X culture volume ice-cold sterile water and centrifuged, and then this step was repeated. Finally, the pellet was resuspended in ice-cold 0.3 M sucrose so that a 1/100 dilution gave OD_{650} between 0.2 and 0.6. These cells were then either used for electroporation or quick frozen in liquid nitrogen and stored at -80 °C until further use.

DNA was introduced into *Pseudomonas* using Gene Pulser cuvettes (BioRad), and a BioRad Gene Pulser electroporator. Capacitance was set to 25 uF, voltage at 1.8 kV, and 200 Ohms of resistance, using a 0.1 cm electrode gap. Growth media was added to the cells and they were incubated at 30 °C with mild shaking for two hours. Finally, aliquots

were plated onto LB plates containing carbenicillin (1000 μg/mL) and grown overnight.

Culture Growth and Induction of DmpF and DmpG Expression

All plasmids derived from pET or pSBET vectors were transformed into *E coli.* BL21 (DE3) (Rosenburg et al, 1987). One colony, from a fresh transformation, was used to inoculate Luria Broth containing either ampicillin (100 μg/ml) for pET vectors, or kanamycin (30 μg/ml) for pSBET vectors: double transformants were grown in the presence of both antibiotics. Cultures were then grown overnight at 37 °C with vigorous shaking. The next morning cells were pelleted at 7,520 x g and resuspended in fresh LB supplemented with the appropriate antibiotic. After a 1/100 dilution, cultures were allowed to grow to OD_{650} 0.6-0.8 at which point, IPTG (0.5 mM) was added to induce expression of the host-encoded T7 polymerase that is under control of the Ptac promoter. After an additional three hours of growth, cells were harvested at 15,300 x g, washed with 20 mM MOPS, pH 7, and stored as paste at -20 °C until further use.

Plasmids derived from the pMMB66 broad-host range vector were propagated in *E. coli* DH5, and electroporated into *Pseudomonas* PB2701 for expression. A colony from a plate obtained after a fresh electroporation was inoculated in LB containing carbenicillin (1000 μg/mL), and allowed to grow for eight hours. At that point 1:1000 dilution was carried out in fresh LB + Cb_{1000} and the culture was grown for sixteen hours. Cells were then harvested at 15,300 x g and stored at -20 °C as a cell paste until further use.

Analytical Methods

Protein Estimation

Protein concentrations were estimated using the BCA protein assay (Pierce Chemical Co.) with bovine serum albumin as the standard. The protocol for 60 °C described by the manufacturer was used, with a modification of the protocol used when dithiothreitol was present (Brown et al, 1989).

Electrophoresis of Protein Samples

Protein samples were either subjected to Tricine SDS-PAGE (Schagger & Von Jagow, 1987) or 16% SDS-PAGE (Laemmli, 1970). Gels were run at 100 V as the samples migrated through the stacking gel and then at 200 V after samples had entered the resolving portion of the gel.

Enzyme Activity Assays

Aldolase Standard Assay

The activity assay for 4-hydroxy-2-ketovalerate aldolase was carried out in a 1.5 mL cuvette at room temperature in the presence of excess lactate dehydrogenase, which reduces pyruvate formed by the action of the aldolase (Sala-Trepat & Evans, 1971; Shingler, Powlowski & Marklund, 1992). Reaction mixtures (1 mL) included, 50 mM Hepes, pH 8, containing $MgCl_2$ (1 mM), NADH (260 μM), either synthetic (racemic mixture) or L- 4-hydroxy-2-ketovalerate (260 μM), pig heart lactate dehydrogenase (25 U) and enzyme. The reaction was initiated by the addition of enzyme.

An Alternative Assay for 4-hydroxy-2-ketovalerate aldolase

This alternative assay was useful for detecting low levels of activities and is not subject to the "background" NADH oxidase activity that the previously described assay suffers from when crude extracts are used. An aliquot (100 μL) of sample containing 4-hydroxy-2-ketovalerate was acidified with HCl (1.5 mL of a 0.3 N solution) and boiled for 3 minutes to convert 4-hydroxy-2-ketovalerate to the lactone, and then cooled on ice. The Absorbance was read at 230 nm where the lactone absorbs strongly with a molar extinction coefficient in acid of 5200 $M^{-1}cm^{-1}$ (Dagley & Gibson, 1965). HPLC analysis was used to check for purity of the lactone.

Dehydrogenase Standard Assay

The assay for acetaldehyde dehydrogenase (acylating) activity, carried out at room temperature in a 1.5 mL cuvette, included 50 mM Na^+ K^+ phosphate, pH 7.5, NAD^+ (285 μM), acetaldehyde (10 mM), and enzyme in a total volume of 1 mL(Shingler, Powlowski & Marklund, 1992). The reaction was initiated by the addition of acetaldehyde. One unit of activity is defined as the amount of enzyme required to catalyze reduction of 1μmol of NAD^+ per minute.

Coupled Assay Using Racemic and L- 4-hydroxy-2-ketovalerate

Coupled assays were performed in order to investigate the possibility of substrate channeling between the two enzymes. All the requirements for the standard aldolase assay were present (assay buffer, 4-hydroxy-2-ketovalerate) along with the NAD^+ and CoA required for dehydrogenase activity. Therefore dehydrogenase activity starting

from 4-hydroxy-2-ketovalerate is monitored at 340 nm. The assay, performed at room temperature, contained 4-hydroxy-2-ketovalerate (260 μM) in assay buffer, NAD^+ (285 μM), CoA (100 μM), and native DmpFG enzyme in a total volume of 1 mL. The reaction was initiated by the addition of enzyme. One unit of activity is defined as the amount of enzyme required to catalyze the reduction of 1μmol of NAD^+ per minute.

Determination of Kinetic Constants

Initial enzymatic rates were converted from Absorbance Units/min to μM/min by using an extinction coefficient of 6220 M^{-1} cm^{-1} for NADH (Dawson et al, 1986), and then used to fit data to the Michaelis-Menten equation using an enzyme kinetics program called Grafit (Erithacus Software). All Lineweaver-Burk plots were obtained by data using Grafit, and then fitted by using linear regression. Kinetic constants such as Km and Vmax were obtained from direct fitting of the Michaelis-Menten equation by non-linear regression.

Chemical Modification of DmpF

A 30 mM solution of iodoacetate (sodium salt) from Sigma was freshly prepared in 1M Tris, pH 8.0 and stored in a microfuge tube in the dark. Native enzyme (100 μg) and an iodoacetate solution (28 mM final concentration) were incubated at room temperature for up to 30 minutes. Samples were removed at different intervals, quenched with a 40 mM solution of DTT (3 μl) and placed on ice. These samples were assayed to determine the relative amounts of the two enzymatic activities. The control reaction contained 1M Tris, (3 μL), pH 8.0, instead of the iodoacetate solution.

Results

Results

Two important questions were addressed by the experiments reported here. First, although it had previously been determined that the dehydrogenase enzyme (DmpF) was active on its own, is this true of the aldolase (DmpG)? Second, does substrate channeling occur between DmpG and DmpF in the native enzyme complex? A purification procedure for the aldolase substrate was developed first, before these questions were addressed, since earlier work had indicated a need for this (Powlowski, Sahlman, & Shingler, 1993).

Purification of 4-hydroxy-2-ketovalerate

Substantially less than expected yields of pyruvate were obtained from 4-hydroxy-2-ketovalerate (60% conversion for the L-isomer, and 30% conversion for the racemic mixture) incubated with the purified native aldolase-dehydrogenase, indicating that generation of aldolase substrate by mild alkaline hydrolysis of the corresponding lactone yields an impure preparation. A purification procedure for 4-hydroxy-2-ketovalerate was therefore developed.

After having tested several chromatographic alternatives, a relatively simple procedure of loading the hydrolyzed mixture onto an octadecyl solid-phase extraction cartridge (washed with methanol and equilibrated with water), proved to be sufficient for removing most of the impurities present in the crude preparation (Figures 6A and 6B). Furthermore, the percent conversion of substrate to product in the standard enzymatic aldolase assay increased to 90% for the biological and 44% for the synthetic substrate.

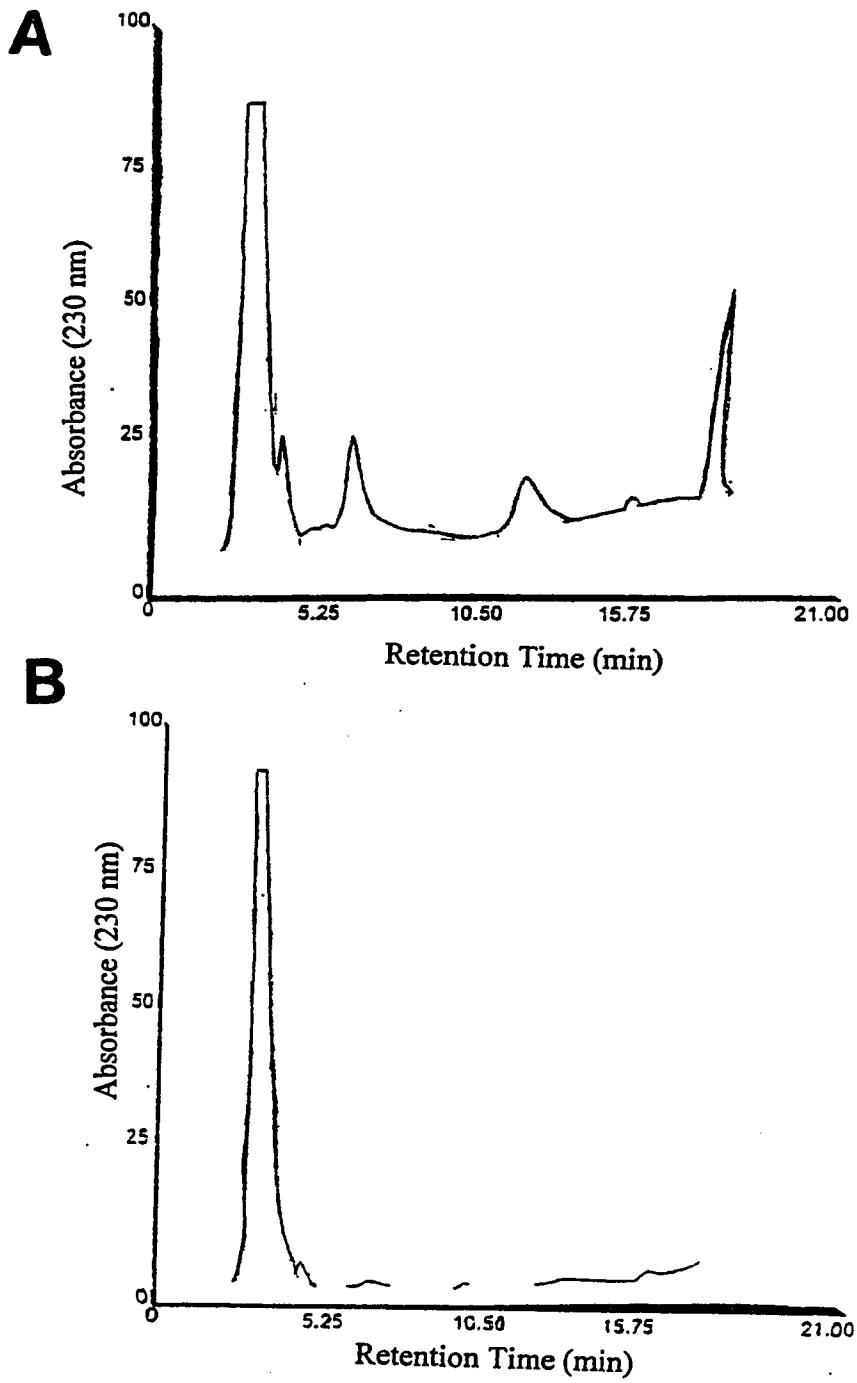

Figure 6: HPLC traces of impure and purified 4-hydroxy-2-ketovalerate. Prior to loading, samples were treated with acid and boiled. Samples remained on ice until they were loaded onto the column. **A:** HPLC trace of impure 4-hydroxy-2-ketovalerate. **B:** HPLC trace of purified 4-hydroxy-2-ketovalerate. Both experiments were carried out as described in *Materials and Methods.*

The difference in biological and synthetic substrate conversions was anticipated, because the enzyme only utilizes the L-isomer of 4-hydroxy-2-ketovalerate (Powlowski, Sahlman & Shingler, 1993).

Expression of DmpG in the Absence of DmpF

It became apparent that the two enzymes needed to be expressed separately, in order to address the first question of whether aldolase (DmpG) is active on its own. Although this had been done previously, expression levels were not particularly high, and only crude extracts were tested for activity, so these experiments were inconclusive (Shingler, Powlowski, & Marklund, 1992). As outlined in the *Materials and Methods* section, *dmpF* and *dmpG* were PCR amplified and cloned into pET3a, a vector used for overexpression using a T7-polymerase dependent promoter (Hanahan, 1985). Expression using this system proved to be problematic, because of the formation of inclusion bodies which were found in the insoluble fraction after sonication (Figures 7A and 7B). Attempts to alleviate inclusion body formation were made, by decreasing the temperature after induction from 37 °C, to 30 °C, 24 °C or 4 °C. Unfortunately these temperatures decreases did not help, and the proteins of interest were still found in inclusion bodies (data not shown).

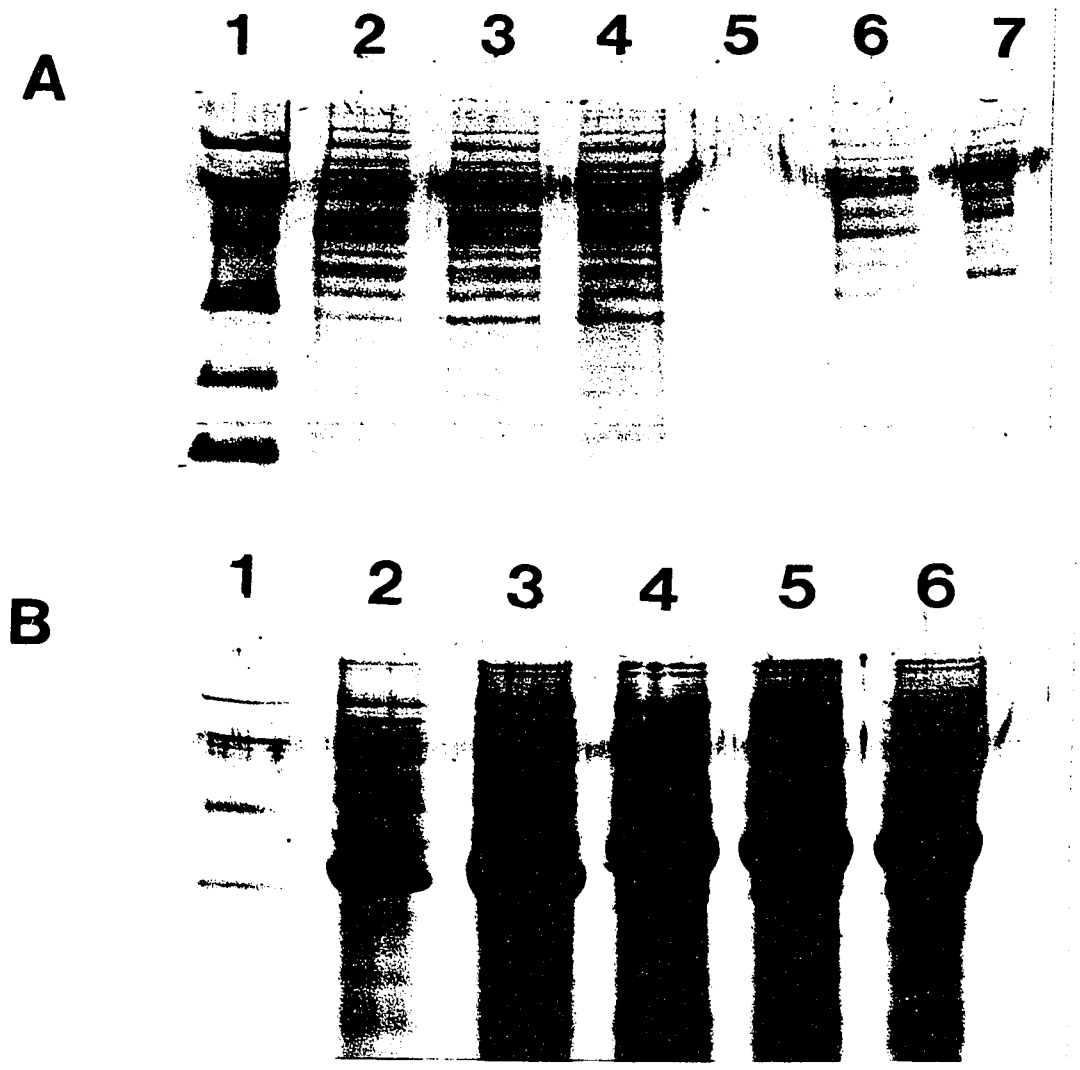

Figure 7: T7-Polymerase mediated expression of DmpF and DmpG in cytosolic (A) and insoluble (B) cell fractions.

A: Tricine gel of soluble proteins expressed in *E.coli* BL21(DE3) harbouring either pET3a (*dmpF*) or pET3a (*dmpG*). Lane 1: molecular weight standards, 94 kDa, 67 kDa, 43 kDa, 30 kDa, 20.1 kDa, and 14.4 kDa. Lanes 2, 3, and 4 contain soluble proteins from cells harbouring pET3a (*dmpG)* cells. Lane 5 is empty and lanes 6 and 7 contain soluble fractions from cells harbouring pET3a (*dmpF*). **B:** Tricine gel of the insoluble fractions from cells indicated in A. Lane 1, molecular weight standards, lanes 2 and 3, contain insoluble proteins from cells harbouring pET3a (*dmpF*), lanes 4, 5, and 6 contain insoluble proteins from cells harbouring pET3a (*dmpG*).

Inclusion bodies were purified using the procedure described in *Materials and Methods*, so that refolding of the insoluble protein could be attempted. After this procedure, relatively pure preparations of DmpF and DmpG were obtained (Figure 8). Purified inclusion bodies were solubilized in 6 M urea and stored at –20 °C, until they were used for dialysis. Preliminary dialysis results indicated that some solubility problems occurred after all the urea was removed from samples. Therefore different conditions were tested in order to determine which one would be best for higher yields of refolded DmpF and DmpG. Dialysis against a neutral buffer of pH 7 resulted in the highest yield of soluble protein with lower yields obtained at pH 6 and pH 8 (Table 2).

Dialysis results indicated that refolded DmpF was active under all conditions (Table 3): it had previously been determined that DmpF is active in the absence of DmpG (Powlowski, Shingler & Marklund, 1992). Attempts to gain aldolase activity were made, by using buffers at pH 7, to help maintain the protein in a soluble form, and by including metals in the dialysis buffers. Aldolase is stimulated by Mn^{+2}, but it is unclear whether it is an effector or needed structurally (Powlowski, Sahlman & Shingler, 1993). EDTA was also added to some of the dialyses in order to chelate any excess metals. The two proteins, DmpF and DmpG, were also dialysed in the same dialysis bag in hopes of reconstituting an active enzyme complex. However, as indicated in Table 3, active aldolase was never recovered.

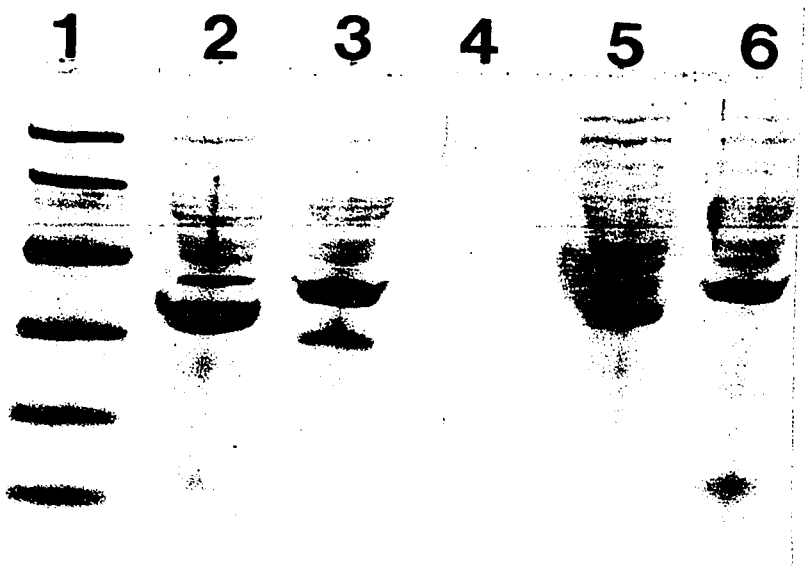

Figure 8: Purified inclusion bodies from cells harbouring either pET3a (*dmpF*) or pET3a (*dmpG*): This Tricine gel contains purified and solubilized inclusion bodies from *E coli* BL21(DE3) cells which harboured either pET3a (*dmpF*), lanes 2 and 5, or pET3a (*dmpG*) lanes 3 and 6. The purification procedure is outlined in the *Materials and Methods* section. The molecular weight markers are in lane 1 and represent, 94, 67, 43, 30, 20.1, and 14.4 kDa.

Table 2: Effects of pH and salt concentration on the yields of soluble refolded DmpG. A number of dialysis conditions for urea solubilized inclusion bodies produced from pET3a (*dmpG*) were set up in order to determine which pH would be the most appropriate for conducting further experiments. DTT and glycerol had already been determined as protein stabilizers (data not shown). Metals included in DmpG preparations had also been proven to stabilize DmpG, but destabilize DmpF.

Dialysis Buffer* **During Refolding**	**Soluble Protein (μg) Before Dialysis**	**Soluble Protein (μg) After Dialysis**	**%Yield**
0.1 M MES, pH 6	100	45	45
0.1 M MES, pH 6, 0.1 M NaCl	100	30	30
0.1 M MOPS, pH 7	100	53	53
0.1 M MOPS, pH 7, 0.1 M NaCl	100	50	50
0.1 M HEPES, pH 8	100	10	10
0.1 M HEPES, pH 8, 0.1 M Nacl	100	40	40

* All dialysis buffers also contained 0.5 mM $MnCl_2$, 0.5 mM $MgCl_2$, 1 mM DTT, and 10% glycerol.

Insoluble protein was removed by centrifugation.

Table 3: Activity assay results for solubilized inclusion bodies:

These dialysis results are a summation of those that yielded the highest amount of soluble refolded protein under different conditions. DmpF and DmpG refer to pET3a *(dmpF)* and pET3a *(dmpG)* respectively.

Sample	Buffer	Activity Detected
pET 3a *(dmpF)*	50 mM Tris pH 7.5	Dehydrogenase
pET 3a *(dmpG)*		None
DmpF + DmpG		Dehydrogenase
pET 3a *(dmpF)*	20 mM MOPS pH 7, 1 mM DTT, 10% glycerol	Dehydrogenase
pET 3a *(dmpG)*		None
DmpF + DmpG		Dehydrogenase
pET 3a *(dmpF)*	20mM MOPS pH 7, 1 mM DTT, 10% glycerol, 1 mM $MgCl_2$, 1mM $MnCl_2$	Dehydrogenase
pET 3a *(dmpG)*		None
DmpF + DmpG		Dehydrogenase
pET 3a *(dmpG)*	20 mM MOPS pH 7, 1 mM DTT, 10% glycerol, 1 mM $MnCl_2$	None
pET 3a *(dmpG)*	As above, but 1 mM $MgCl_2$	None
pET 3a *(dmpG)*	As above, but $MgCl_2$, EDTA, 500 uM	None
pET 3a *(dmpG)*	As above, but $MnCl_2$, EDTA, 500 uM	None

Coexpression of DmpF and DmpG

A new strategy was designed to overexpress the two proteins in *E. coli* concurrently in the hopes that active recombinant DmpG could be recovered. In order for this expression system to be used, *dmpG* and *dmpF* were introduced into a plasmid compatible with pET3a based plasmids. The two genes were cloned into pSBET vectors that contain a different origin of replication than the pET3a vector. After coexpression, inclusion body formation was once again observed (data not shown).

Independent Expression of DmpF and DmpG in Pseudomonas

Considering the fact that both proteins are native to *Pseudomonas*, expression of each protein separately was attempted in *Pseudomonas* PB2701, which lacks the genes encoding the *meta*- cleavage pathway. When DmpF and DmpG were expressed together constitutively from the pMMB66Δ broad host range vector in *Pseudomonas* PB2701, most of the DmpF and DmpG appeared in the insoluble fraction (Figure 9, lanes 2 and 3). When expressed in *E. coli* from the same plasmids, similar results were obtained (Figure 9, lanes 4 and 5). Background levels of contaminating proteins were also very high. When DmpF was expressed alone in *Pseudomonas* most of the protein appeared to be associated with the insoluble fraction (Figure 9, lanes 6 and 7). DmpG expressed alone in *Pseudomonas* appears to be soluble form, at quite a high level (Figure 9, lanes 8 and 9). Note the absence of a band migrating in this position in the construct expressing DmpF.

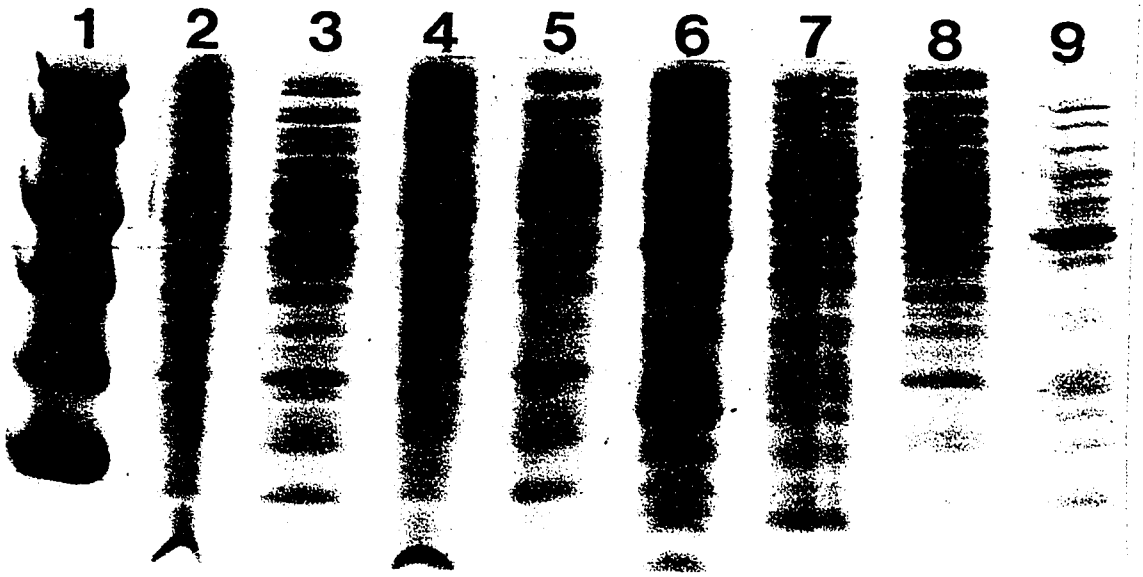

Figure 9: Expression of *dmpF* and *dmpG* in *Pseudomonas* PB2701. Soluble and insoluble cell fractions were loaded onto a Tricine gel. The samples were run at 100 V as they migrated through the stacking gel and 150 V as they migrated through the resolving portion of the gel. Lane 1, molecular weight markers, 94, 67, 43, 30, 20.1, and 14.4 kDa, lane 2, insoluble fraction of *Pseudomonas* PB2701 harboring a pMMB66 vector coexpressing DmpF and DmpG, lane 3, soluble fraction of *Pseudomonas* PB2701 harboring a pMMB66 vector coexpressing DmpF and DmpG, lane 4, insoluble fraction of *E. coli* BL21(DE3) harboring a pMMB66 vector coexpressing DmpF and DmpG, lane 5, soluble fraction of *E. coli* BL21(DE3) harboring a pMMB66 vector coexpressing DmpF and DmpG, lane 6, insoluble fractions of *Pseudomonas* PB2701 cells harboring PVI310 (DmpF), lane 7, soluble fractions of *Pseudomonas* PB2701 cells harboring PVI310 (DmpF), lane 8, insoluble fractions of *Pseudomonas* PB2701 harboring PVI312 (DmpG), and lane 9, soluble fractions of *Pseudomonas* PB2701 harboring PVI312 (DmpG).

The soluble *dmpG* gene product was purified from *Pseudomonas* PB2701 harbouring pVI310 (Figure 10). Cells from 3 L of culture were used for purification, which was carried out as described in *Materials and Methods.* This yielded 7 mg of pure protein. The protein was approximately 95% pure as estimated by SDS-PAGE (Figure 10 lanes 2, 3, 4 and 5).

Purified DmpG was used in the same standard aldolase assay as the native DmpFG complex, but contaminants precipitated out of solution upon addition of the purified protein to the assay buffer, which made the spectrophotometric assay impossible to interpret. What appeared to be happening was that the Mn^{+2} in the assay buffer was complexing with some of the contaminants in the DmpG preparation, and these complexes were precipitating out of solution. SDS-PAGE confirmed that upon the addition of 15 ug of pure DmpG to an assay mixture, only 0.5 ug of protein was precipitated out of solution (Pierce BCA Protein Assay). These precipitated proteins all corresponded to a fraction of the contaminants seen in the purified aldolase preparation (data not shown).

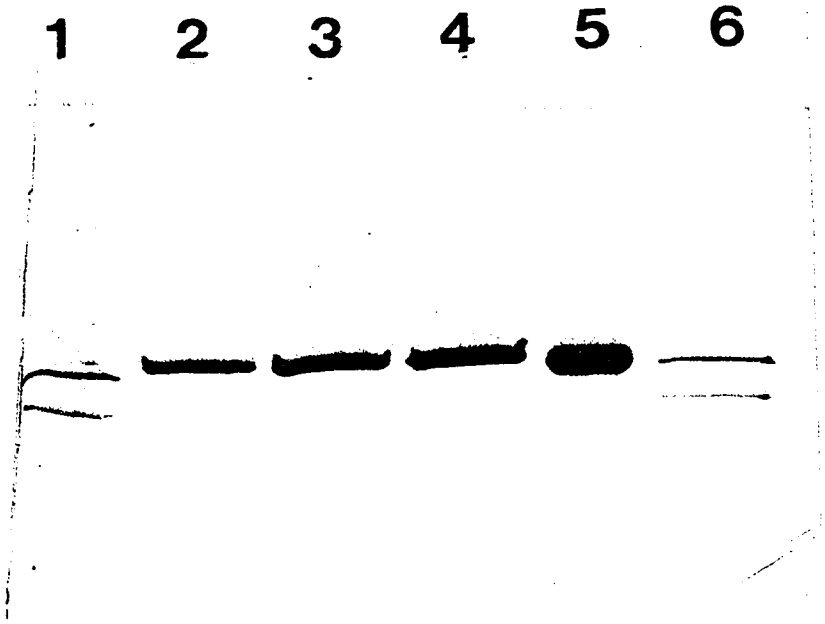

Figure 10: Electrophoretic comparison of DmpG purified from *Pseudomonas* PB2701 and the DmpFG complex from *Pseudomonas* sp strain CF600.

A 10-20% acrylamide gradient gel was run at 220V. DmpG is the upper band in the complex. Lanes 1 and 6 contain 1 μg of purified native DmpFG. Lanes 2, 3, 4, and 5 contain 1.5, 3, 4.5 and 6 μg of purified DmpG.

An alternative method for assaying the aldolase, outlined in *Materials and Methods*, was used in order to circumvent the precipitation problem. These assays were performed in order to confirm whether or not the aldolase preparation was active (Figure 11). What was expected in the case of active protein was a decrease in the NADH concentration, and consequently a decrease in the absorbance at 340 nm, which would correspond to the reduction of pyruvate to lactate by the coupling enzyme, lactate dehydrogenase. In addition to the coupled assay, a direct assay for the substrate, 4-hydroxy-2-ketovalerate was performed by converting it back to its corresponding lactone, which was then quantitated by its Absorbance at 230 nm. In this case, a decrease in the absorbance at 230 nm should have also been observed if the aldolase protein was active. The results shown in Figure 11 indicate that the preparation of DmpG obtained was inactive.

Steady State Kinetics of the DmpFG Complex:

Aldolase Activity:

The steady-state kinetics of the two activities of the native protein were examined in order to determine a kinetic mechanism. Comparison of the kinetic parameters for the individual and overall reaction was also necessary in order to determine whether substrate channeling actually occurs between the two enzymes. For this, the uncoupled and coupled reactions for each enzyme have to be kinetically elucidated and compared with one another.

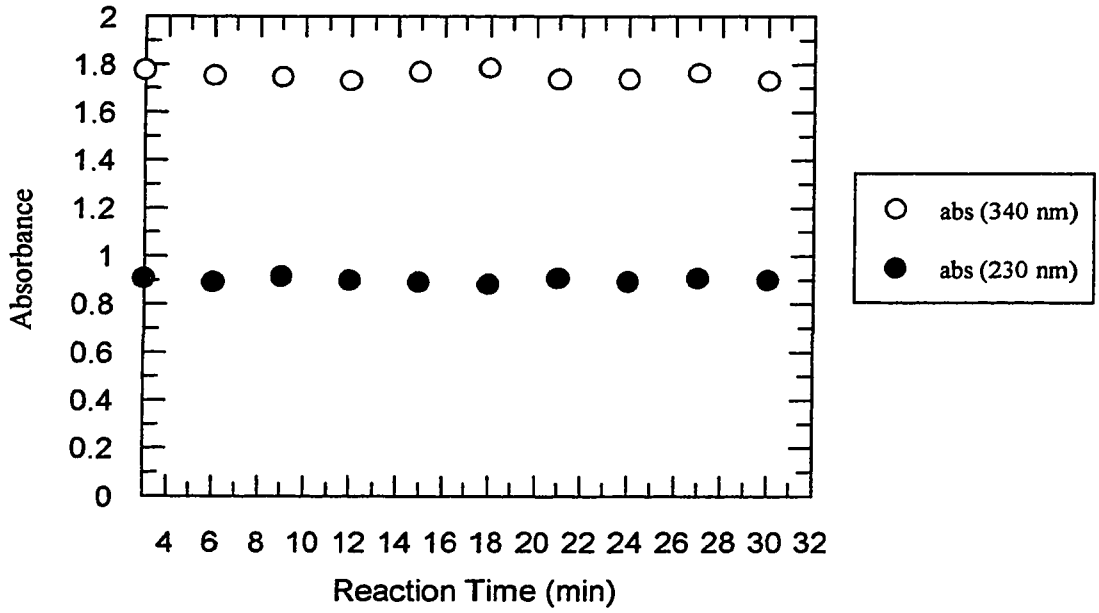

Figure 11: Aldolase activity of purified DmpG. Assays were performed with 15 ug of pure DmpG as cited in the *Materials and Methods*. After initiation of the enzymatic assays, precipitate was removed by centrifugation. The absorbance at 340 nm monitors the conversion of NADH to NAD^+, through the action of LDH in the coupled assay for aldolase. Parallel aldolase assays were also executed which did not contain LDH or NADH. These samples were boiled in acid, to convert the 4-hydroxy-2-ketovalerate to its corresponding lactone and cooled on ice. The absorbance of the lactone at 230 nm was measured.

Assay of aldolase activity was carried out either by coupling to acetaldehyde dehydrogenase (DmpF), or to lactate dehydrogenase (Figure 12). In these experiments the biologically active isomer, L-4-hydroxy-2-ketovalerate, was used as substrate. Data fitting revealed a $kcat_{app}$ of 580 min^{-1} for the reaction coupled with ALDH. This value was 108 min^{-1} when the reaction was coupled to LDH. The plateau that is reached in Figure 12 for the reaction coupled with LDH was not due to a limitation in the LDH coupling enzyme. The rate observed was the maximal rate possible for the reaction, because inclusion of a higher concentration of LDH (3X) did not alter the observed rate. The apparent Km values for L- 4-hydroxy-2-ketovalerate measured in the two reactions were also different, 97 μM for the assay coupled to ALDH, and 9.6 μM for the LDH coupled reaction.

The kinetic analysis was also performed using racemic 4-hydroxy-2-ketovalerate. These results are illustrated in Figure 13. Both reactions were significantly slowed, to approximately the same rate as that observed for the coupled LDH reaction using L-4-hydroxy-2-ketovalerate (Figure 12). Kinetics with the native aldolase enzyme were also performed in the presence of varying metal concentrations. The results are shown in Figure 14. This data confirms that the Mn^{+2} concentration is saturating in the standard assay buffer used for all of the aldolase assays.

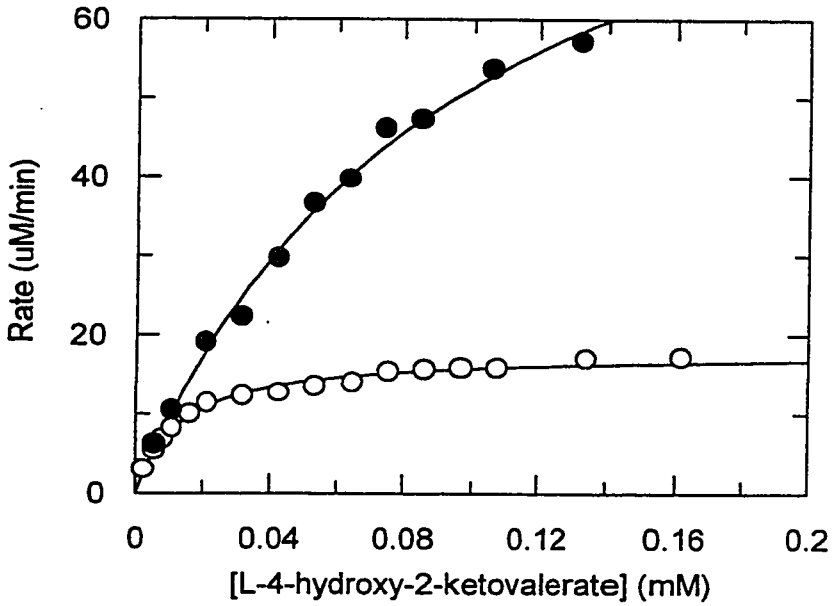

Figure 12: Rate vs substrate concentration for turnover of L-4-hydroxy-2-ketovalerate by the native DmpFG enzyme. The reaction coupled with LDH, O, is the standard assay to detect aldolase activity described in *Materials and Methods*. The reaction coupled with the *dmpF*-encoded dehydrogenase, ●, is also described in *Materials and Methods*. Both reactions were carried out in assay buffer at room temperature. The solid lines represent fits of the data to the Michaelis-Menten equation using the program GraFit (Erithacus Software).

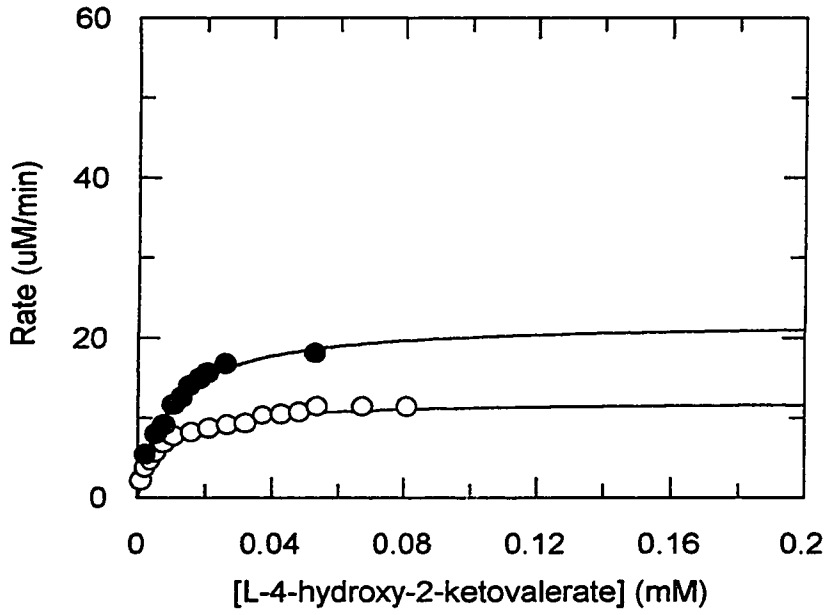

Figure 13: Rate vs substrate concentration for turnover of D, L- 4-hydroxy-2-ketovalerate. The two different coupled assays are as outlined in *Materials and Methods*. For comparison purposes the axes on this graph are the same as those in Figure 15. O, reaction coupled with LDH and ●, reaction coupled with ALDH. The solid lines represent fits of the data to the Michaelis-Menten equation using the program GraFit (Erithacus Software).

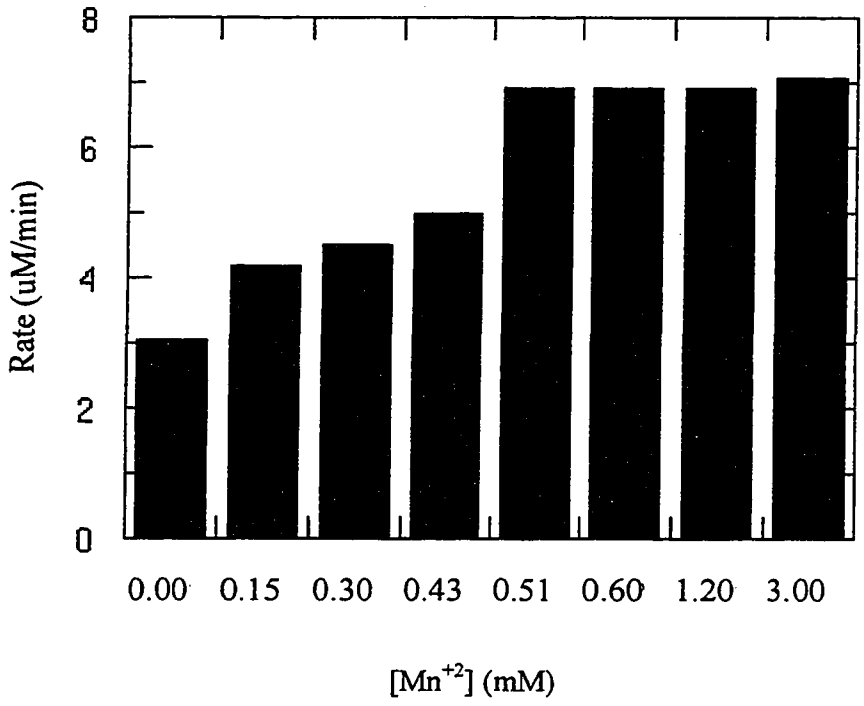

Figure 14: Stimulation of aldolase activity by increasing manganese concentrations. Rate vs metal concentration for the coupled LDH assay used to monitor aldolase activity. Assays were performed as outlined in *Materials and Methods*. The Mn^{+2} concentration in the standard assays was 1 mM.

Steady State Kinetics of the DmpFG Complex

Kinetic Mechanism of DmpF

Initial rate plots can be used as a diagnostic tool in interpreting the kinetic mechanism of enzymes. For a three substrate reaction, the kinetic mechanism can either be "sequential", in which all the substrates bind prior to the release of products, or "ping-pong" in which the binding of substrates is interrupted by the release of a product (Segel, 1975). A sequential mechanism leads to intersecting lines on initial rate plots, while a ping-pong mechanism gives one or more parallel plots. Fromm originated the method used here to probe the kinetics of the dehydrogenase enzyme (DmpF) in the complex. In this method, two substrates are held at a constant ratio at different concentrations, while the third substrate is varied. This process is repeated for all three substrates, and once a complete set of plots has been obtained, not only can ping-pong and sequential mechanisms be distinguished, but also subclasses of these two mechanisms may be defined (Segel, 1975).

Subclasses of sequential and ping-pong mechanisms are distinguished by the slope and y-intercept replots of initial rate plots. Y-intercept replots are directly associated with maximum velocity measurements at the different concentrations, while slope replots reflect the change in rates associated with the different constant ratio two substrate concentrations. At low, fixed ratio substrate concentrations, slopes have higher numeric values than those which are obtained at higher concentrations of the two, fixed ratio, substrates.

When acetaldehyde was used as the varied substrate and NAD^+ and CoA were kept at constant ratios relative to one another, the results in Figure 15 were obtained. On the double reciprocal plot all the lines intersect at a Km_{app} of 50 mM. The y-intercept and slope replots for the initial rate kinetics data obtained by varying the concentration of acetaldehyde in Figure 15 are shown in Figure 16 and Figure 17.

Double reciprocal plots with NAD^+ as the varied substrate were also obtained (Figure 18). CoA and acetaldehyde concentrations were kept at a constant ratio relative one another. All but one of the double reciprocal plots intersect at a similar Km_{app} of 100 µM. The lowest concentration plot intersects at a Km_{app} of 120 µM. Y intercept and slope replots are shown in Figures 19 and 20.

Lineweaver-Burk plots where CoA was the varied substrate also show a pattern of intersecting lines (Figure 21). In this case all of the plots intersect on the y-axis, indicating a Vmax of 5.5 µM/min. The fact that all of the lines intersect at the same y-intercept rules out all but two kinetic mechanisms for sequential binding; (Segel, 1975) the equilibrium ordered terreactant system (Figure 23A) and the random A B, ordered C mechanism (Figure 23B). Ping–pong mechanisms are completely eliminated because ***all*** of the initial rate plots yield sets of intersecting lines.

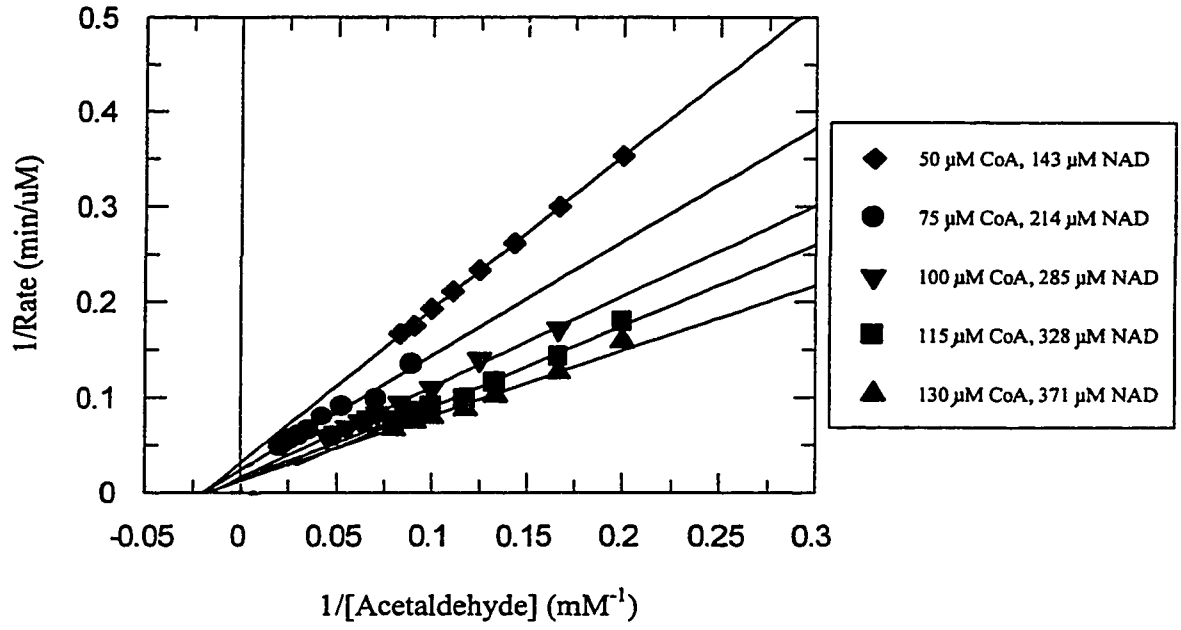

Figure 15: Lineweaver-Burk plots with acetaldehyde as the varied substrate.

For all these plots the CoA and NAD^+ concentrations were kept at a constant ratio relative to one another, as indicated. The solid lines represent data fitted by linear regression analysis using Grafit (Erithacus Software).

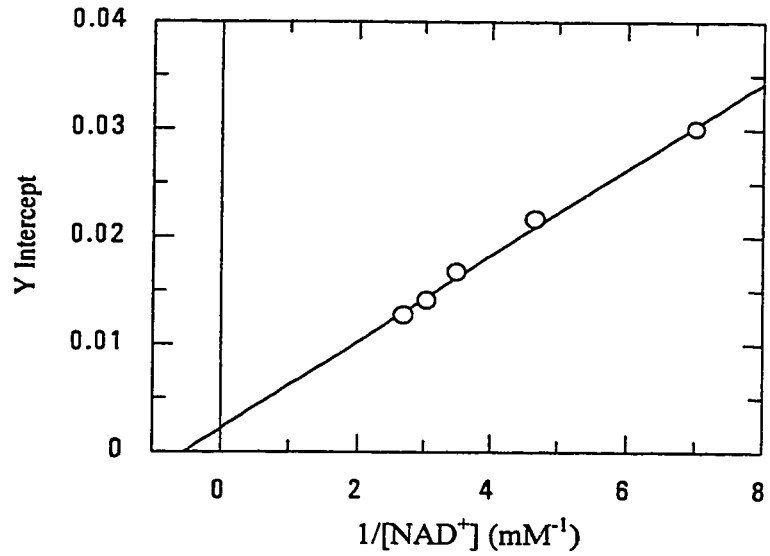

Figure 16: Y-intercept replot with acetaldehyde as the varied substrate. Points are those obtained from the graph shown in Figure 15. The solid line represents fits to the data using linear regression analysis on Grafit (Erithacus Software).

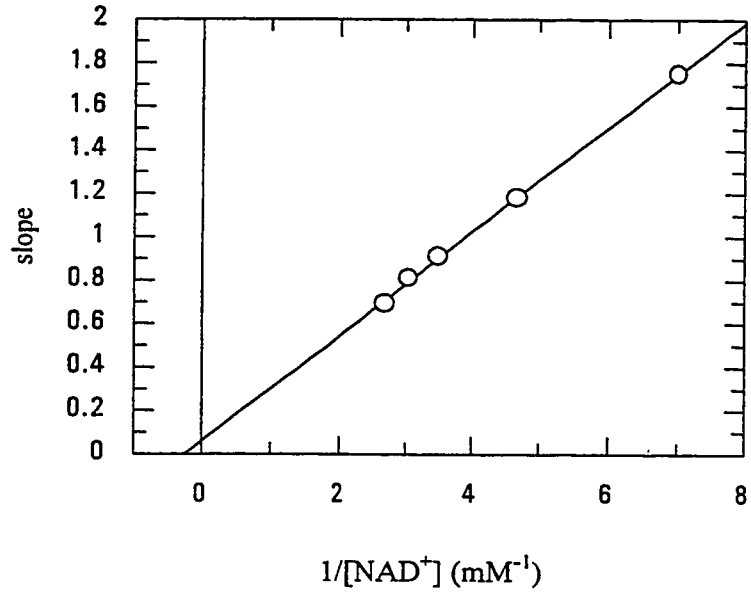

Figure 17: Slope replot with acetaldehyde as the varied substrate. Points are those obtained from the graph shown in Figure 15. The solid line represents fits to the data by linear regression analysis using Grafit (Erithacus Software).

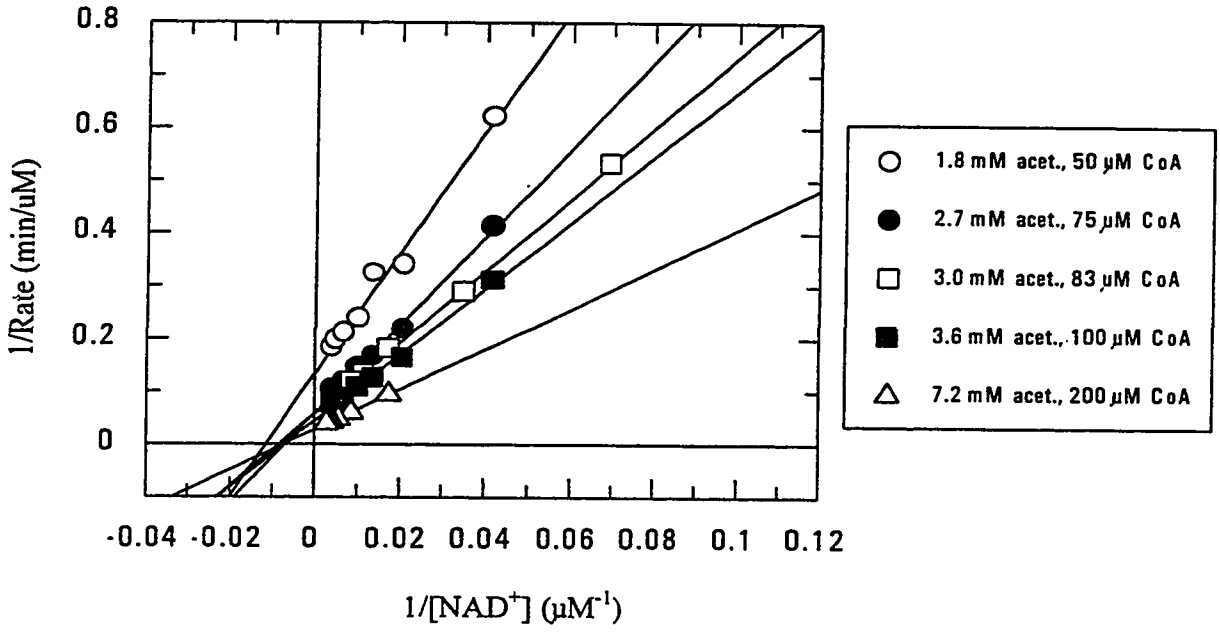

Figure 18: Lineweaver-Burk plots with NAD^+ as the varied substrate:

For all these plots, the acetaldehyde and CoA concentrations were kept at a constant ratio relative to one another, as indicated. The solid curves are fits to the data using linear regression analysis with Grafit (Erithacus Software).

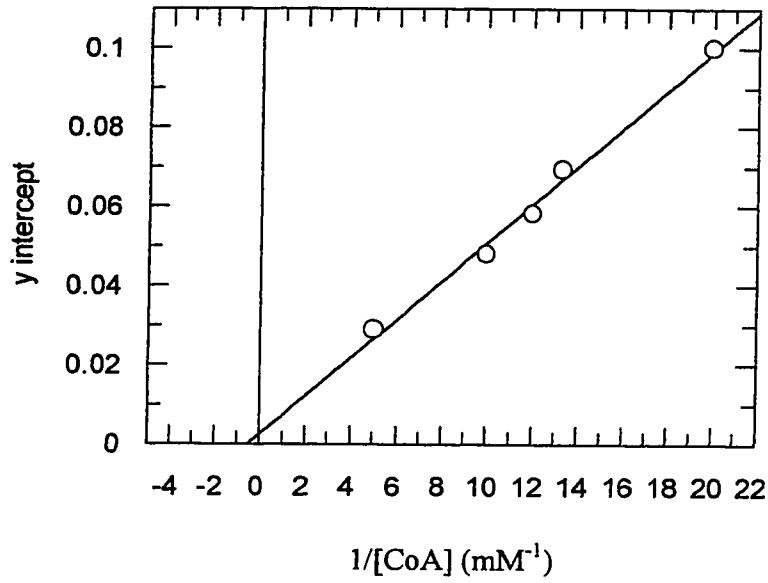

Figure 19:Y-intercept replot with NAD^+ as the varied substrate. Points are those obtained from the graph shown in Figure 18. The solid line represents fits to the data using linear regression analysis with Grafit (Erithacus Software).

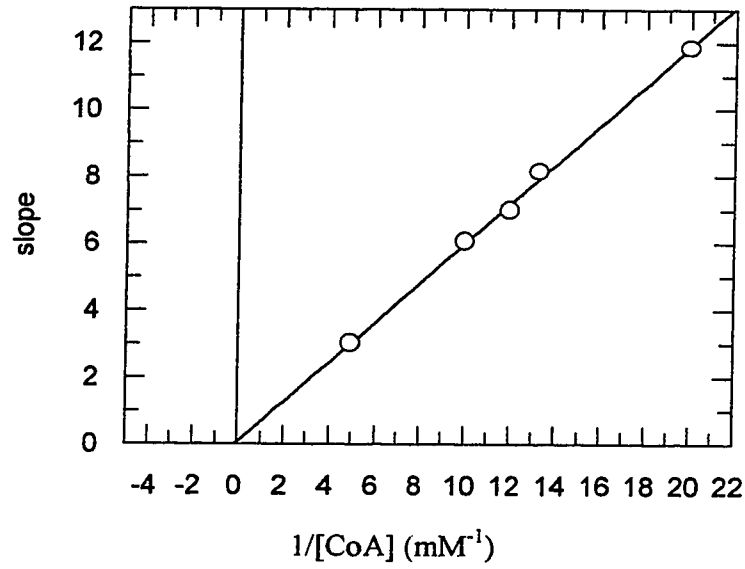

Figure 20: Slope replot with NAD^+ as the varied substrate: Points are those obtained from the graph shown in Figure 18. The solid line represents fits to the data using linear regression analysis with Grafit (Erithacus Software).

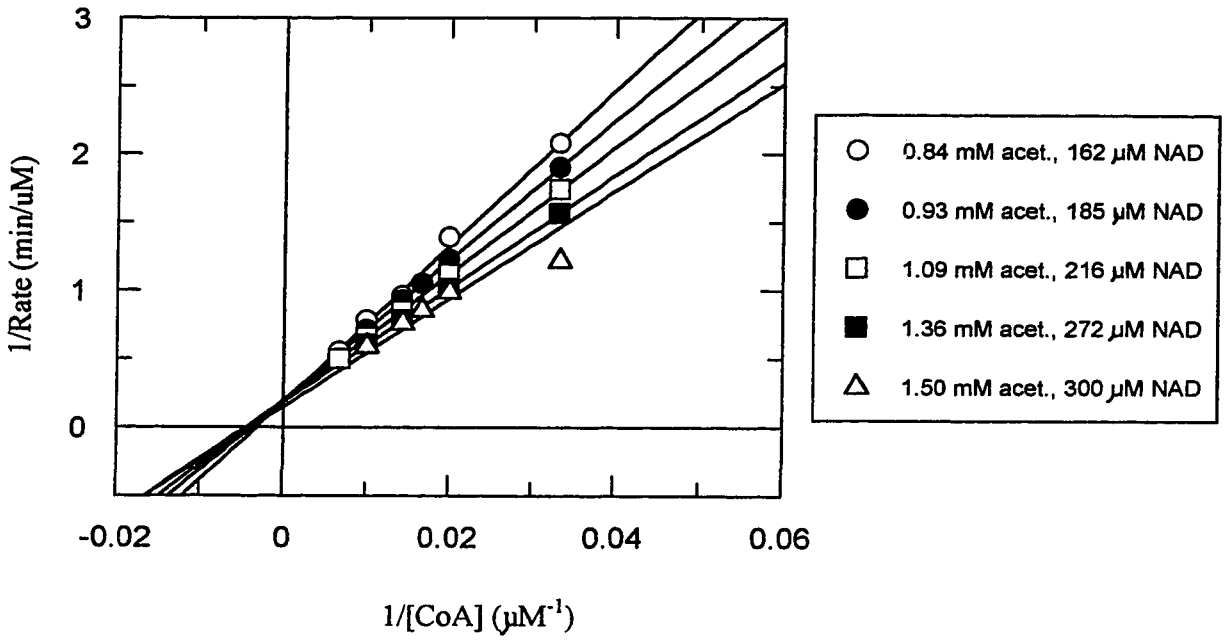

Figure 21: Lineweaver-Burke plots with CoA as the varied substrate:

For all these plots, NAD^+ and acetaldehyde concentrations were kept at a constant ratio relative to one another. The solid lines represent fits to the data using linear regression analysis with Grafit (Erithacus Software).

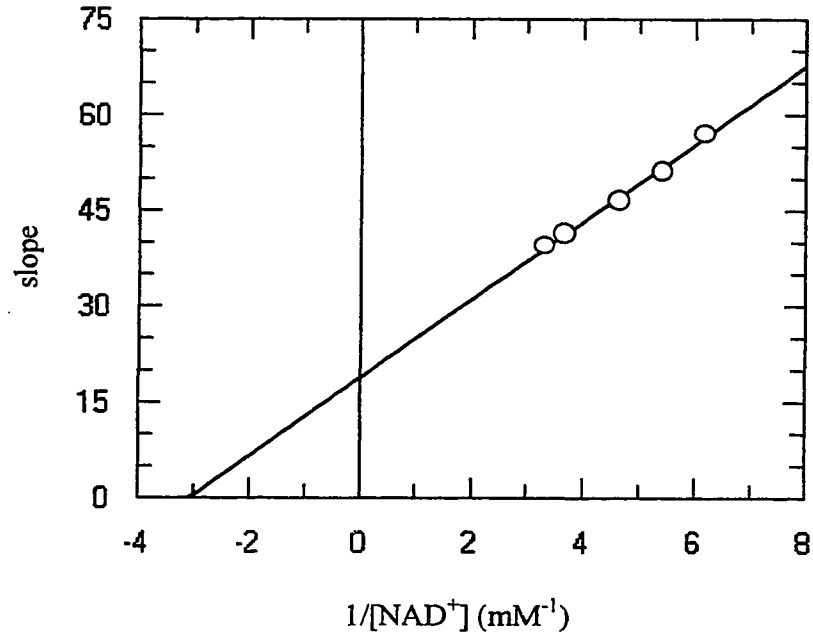

Figure 22: Slope replot of initial rate enzyme kinetics: Points are those obtained from the graph shown in Figure 21. The solid line represents fits to the data using linear regression analysis with Grafit (Erithacus Software).

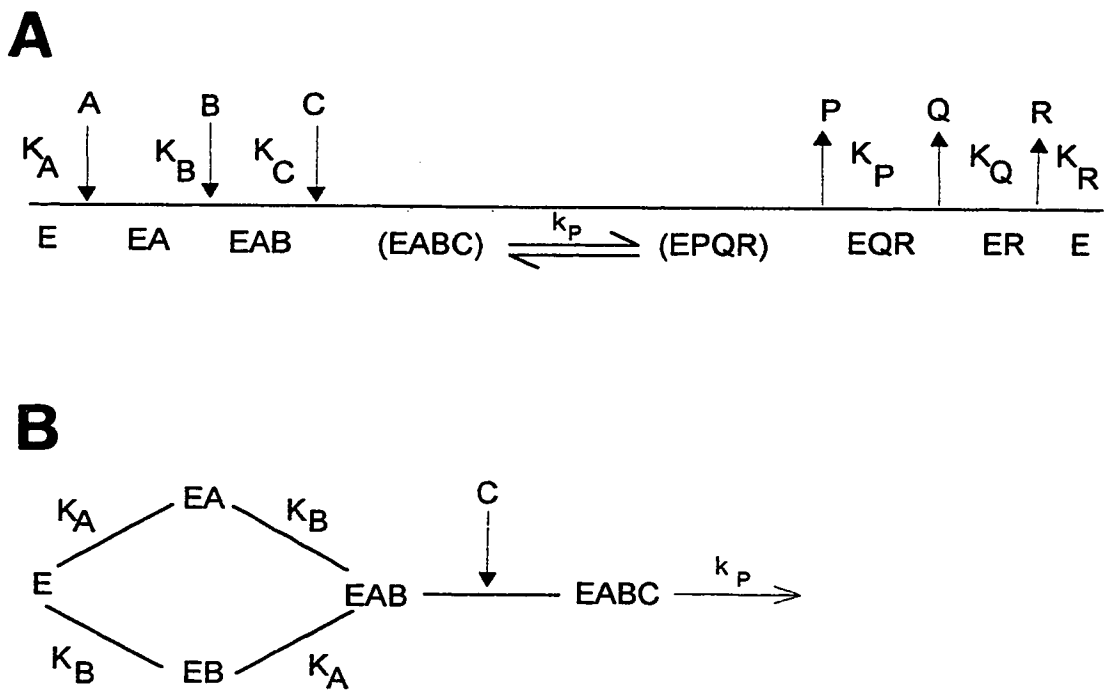

Figure 23: The two possible kinetic mechanisms for the dehydrogenase reaction in the native complex. Both mechanisms are consistent with the observed results. **A:** completely ordered terreactant system: A, B, and C designate acetaldehyde, NAD^+, and CoA, respectively. **B:** Hybrid random terreactant system: A, B, and C designate acetaldehyde, NAD^+, and CoA respectively. K represents binding constants, and k rate constants.

Chemical Modification of DmpF

Relatively high concentrations of acetaldehyde were used in the DmpF assay since the apparent Km for this substrate is approximately 50 mM (Figure 15). At very high levels of acetaldehyde, severe inhibition of the dehydrogenase was observed (Figure 24). The severity of inactivation was dependent on the concentration of the other two substrates, NAD^+ and CoA. As the concentration of these two substrates was increased, protection against inhibition by acetaldehyde was observed (Figure 24).

Cysteine residues have been implicated as active site residues in various aldehyde dehydrogenases, as described in the *Introduction*. Acylating dehydrogenases such as DmpF may thus also contain an active-site cysteine residue. Only two cysteines are present in the nucleotide sequence of the DmpF enzyme (Cys 112 and Cys 132) and only one of them is conserved (Cys 132) (Table 4). Therefore a chemical modification experiment was conducted with the cysteine-directed reagent, iodoacetate (Figure 25). Iodoacetate renders thiols inactive, by acetylation and imparting a negative charge on these residues (Creighton, 1993). Dehydrogenase activity was abolished within the first thirty seconds of exposure to iodoacetate. The aldolase activity on the other hand retained approximately 80% of the control activity (Figure 25).

Table 4: Multiple sequence alignment of DmpF to homologous proteins using Clustal.

DmpF, acetaldehyde dehydrogenase (acylating), *Pseudomonas putida*, **COLI**, acetaldehyde dehydrogenase (acetylating), *E. coli*, **KKS10**, acetaldehyde dehydrogenase (acylating), *Pseudomonas sp.* (strain KKS102), **PUTID**, acetaldehyde dehydrogenase (acylating), *Pseudomonas putida*, **PTWO**, acetaldehyde dehydrogenase (acylating), *Pseudomonas putida*, **FLUOR**, acetaldehyde dehydrogenase (acylating), *Pseudomonas fluorescens*, **PFIVE**, acetaldehyde dehydrogenase, *Pseudomonas putida*, **ALCAL**, acetaldehyde dehydrogenase (acylating), *Pseudomonas pseudoalcaligenes*, **Tol**, acetaldehyde dehydrogenase (acetylating) *Pseudomonas putida* TOL plasmid pWWO, **PTHRE**, acetaldehyde dehydrogenase, *Pseudomonas putida*, **PFOUR**, acetaldehyde dehydrogenase, *Pseudomonas putida*, **ACIN**, acetoaldehyde dehydrogenase, *Acinetobacter sp.*, **UNKN**, unknown, *Mycobacterium tuberculosis*. The two cysteine residues are designated by (*), and as can be seen, only the second one is conserved.

```
DmpF  FDATSASAHVQNEALLRQAKPGIRLIDLTPAAIGPYCVPVVN LEEHLGKE--NVNMVTCGGQA
COLI  FDATSAGAHVKNDAALREAKPDIRLIDLTPAAIGPYCVPVVN LEANVDQL--NVNMVTCGGQA
KKS10 FDATSAGAHVKNDALLRHHKPAMRVIDLTPAAIGPYCIPVVN GEDHLAAL--NVNMVTCGGQA
PUTID FDATSAGAHVKNEALLRERKPGLRMIDLTPAAIAPYCIPVVN GDDHLDAT--NVNMVTCGGQA
PTWO  FDATSAGAHARHEQLLRPH--GVRVIDLTPAAIGPFVVPAVN IEQHLDAP--NVNMVTCGGQA
FLUOR FDATSAYVHAENSRKLNEL--GVMMIDLTPAAIGPFCVPPVN LLKHVGQGEMNVNMVTCGGQA
PFIVE FDATSAYVHAENSRKLNEL--SVMMIDLTPAAIGPFCVPPVN LLKHVGQRELNVNMVTCGGQA
ALCAL FDATSAYVHADNSRKVNAL--GALMIDLTPAAIGPFCVPTVN LKEHVGKGEMNVNMVTCGGQA
Tol   FDATSAYVHAENSRKLNAL--GVLMVDLTPAAIGP-CVPPVN LKQHVGRLEMNVNMVTCGGQA
PTHRE FDATSAYVHAENSRKLNAL--GVLMVDLTPAAIGPYCVPPVN LKQHVGRLEMNVNMVTCGGQA
PFOUR FDATSAYVHAENSRKLNAL--GVLMVDLTPAAIGPYCVPPVN LKQHVGRLEMNVNMVTCGGQA
ACIN  FDATSAYVHAENSRKLNEL--GVIMIDLTPAAVGPFCVPPVN LTDHAKNLEMNVNMVTC-VPS
UNKN  FEATSAYVHRDAAPKYAEA--GIRAIDLTPAAVGPAVIPPAN LREHLDAP--NVNMITCGGQA
                                                 *                  *
```

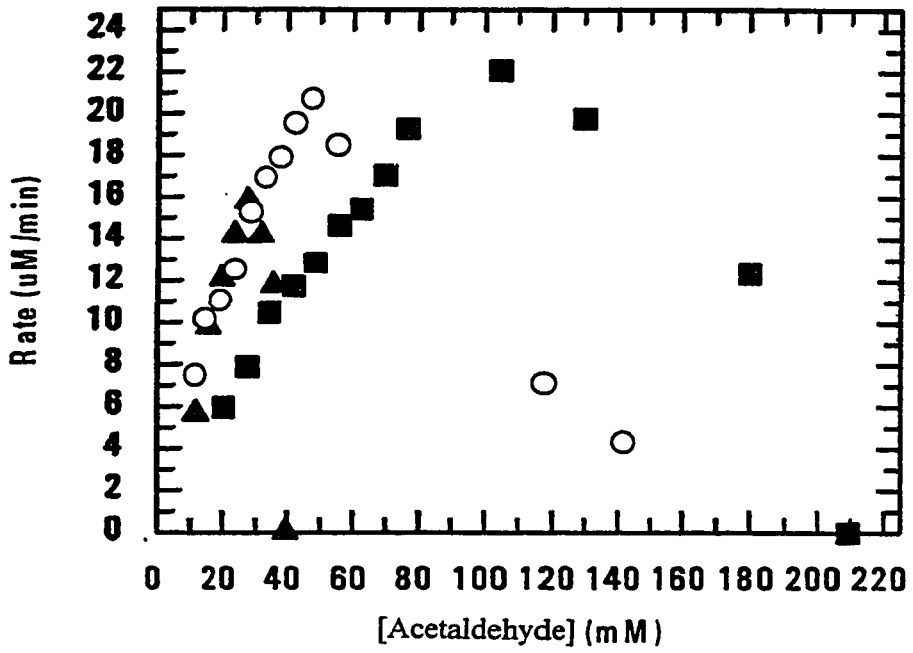

Figure 24: Inhibition of native DmpFG by acetaldehyde and substrate protection from NAD^+ and CoA: Inhibition of native DmpFG by high concentrations of acetaldehyde, at varying concentrations of NAD^+ and CoA. O, 75 uM CoA, 214 uM NAD^+; ■, 130 uM CoA, 371 uM NAD^+; and ▲, 30 uM CoA, and 86 uM NAD^+.

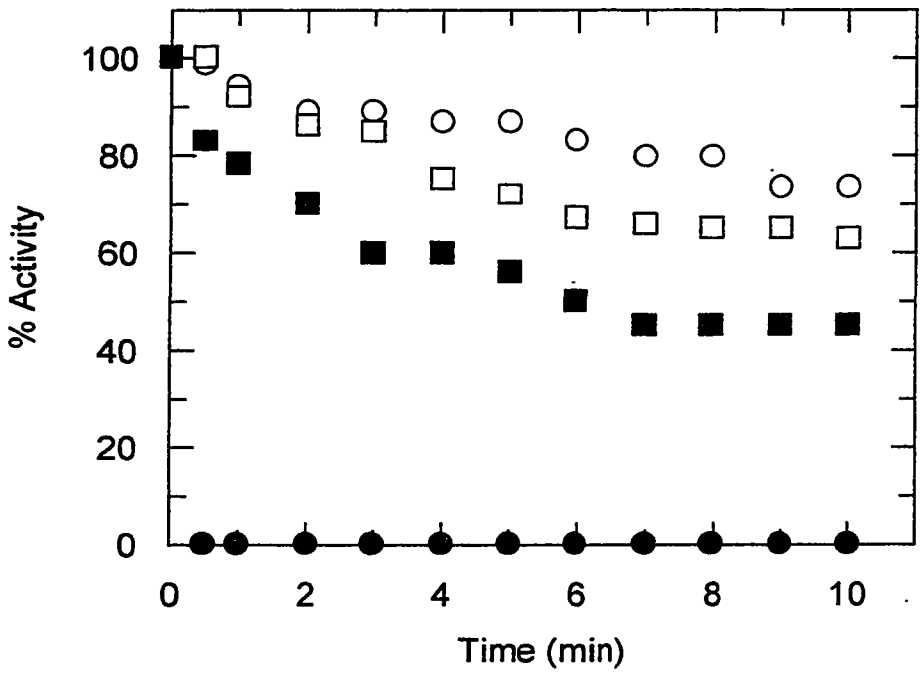

Figure 25: Chemical modification of the wild-type enzyme with iodoacetate: Chemical modification of native DmpFG by iodoacetate, and its effect on aldolase and dehydrogenase activities. The specific assay and modification conditions are as described in *Materials and Methods.* O, dehydrogenase activity in control lacking iodoacetate, ●, dehydrogenase activity in reaction mixture containing iodoacetate, □, aldolase activity in reaction mixture lacking iodoacetate, and, ■, aldolase activity in the presence of iodoacetate.

Discussion

Discussion

The work reported in this thesis was mainly intended to answer two important questions about the native DmpFG complex. First, DmpG (aldolase) was overexpressed independently of DmpF and purified in an attempt to determine whether this polypeptide alone possesses aldolase activity. Secondly, steady-state enzyme kinetics were used in order to address the question of coupling and metabolite channeling between aldolase and aldehyde dehydrogenase (acylating) active sites. In addition, observations were made regarding: modification of the native enzyme by acetaldehyde; substrate protection against aldehyde modification by CoA and NAD^+; metal dependence of the aldolase reaction; and the kinetic mechanism of the DmpF (dehydrogenase) enzyme. Another very important finding implicated a cysteine residue in the dehydrogenase, but not aldolase, catalytic activity.

As has been reported previously (Powlowski, Sahlman & Shingler, 1993, and references therein) impure preparations of 4-hydroxy-2-ketovalerate were obtained using mild alkaline hydrolysis of the corresponding lactone (Dagley & Gibson, 1965). For the work in this thesis, a purification method using an octadecyl solid phase extraction cartridge was developed before proceeding to kinetic studies. The results indicated that the cartridge removed a significant portion of the contaminants, as was confirmed by HPLC analysis. This method is very simple, because it only requires that the sample be washed through the column. The contaminants bind to the nonpolar resin of the cartridge, while the substrate washes through.

One hundred percent conversion of 4-hydroxy-2-ketovalerate to pyruvate and then lactate in the standard aldolase assay was not observed even after purification of the substrate; yields were about 90%. This may indicate that the hydrolysis of lactone to 4-hydroxy-2-ketovalerate reaches a state of equilibrium, in which not all of the lactone gets converted to 4-hydroxy-2-ketovalerate. Using up all of the 4-hydroxy-2-ketovalerate in the equilibrium will not pull the rest of the lactone to the open form when assaying for aldolase activity, because the conditions are no longer ideal for lactone conversion to product. The purer preparation was beneficial in performing enzymatic assays and allows for a more realistic study of the enzymatic action of the aldolase since contaminant levels appear to be very low in the purified samples (Figure 6B).

Although the two proteins, DmpF and DmpG, had already been expressed independently from a pMMB66Δ broad host range expression vector, expression of *dmpG* alone did not yield any aldolase activity (Shingler, Powlowski, & Marklund, 1992). In these experiments, activity results were obtained using crude extracts, so the lack of activity may have been due to low expression levels or interference in the assay by other proteins in the crude extract. In fact, work reported here indicates that when DmpG is expressed independently in *E. coli*, it tends to form inclusion bodies. Therefore these earlier experiments were inconclusive. However, aldolase activity *was* found in strains that coexpressed *dmpF* and *dmpG*. This led the authors to postulate that the aldolase activity was dependent on the presence of dehydrogenase activity (Shingler, Powlowski & Marklund, 1992). In the hopes of getting a clearer answer to the question of DmpG's competence in catalyzing the aldolase reaction, a new expression system was formulated

for the overexpression of soluble DmpF and DmpG. Once this goal had been achieved for DmpG, the protein was purified for activity assays.

The pET system is a high yield, IPTG inducible expression system. It is not uncommon for the protein encoded by the cloned gene to make up 10-50% of the total protein produced by the cells (Creighton, 1993). With such high levels of expression of the protein of interest, the purification protocols can be considerably simplified. Other proteins from *Pseudomonas* sp strain CF600 had already been successfully expressed using this system so it was a reasonable alternative for the overexpression of DmpF and DmpG.

Unfortunately in this system and several others tested, inclusion bodies were a persistent problem (Figures 7, 8 and 9). A direct answer as to why inclusion body formation could not be avoided is not known. Inclusion body formation normally results from proteins being misfolded, although why proteins accumulate in this way is not completely known (Creighton, 1993). Some important factors that favor inclusion body formation appear to be the high concentrations of quickly synthesized protein and the relative insolubility of unfolded polypeptides, which aggregate before they can fold to a more soluble form (Creighton, 1993). Considering the fact that the aldolase (DmpG) – dehydrogenase (DmpF) complex contains two polypeptides of each protein, the contacts formed between each polypeptide may be highly hydrophobic. Contacts become exposed when expressed in the absence of the normal polypeptide partner and polypeptides could associate with themselves leading to a preparation of amorphous aggregates of the synthesized protein

with other cellular components. It should be noted here that inclusion body formation was monitored from the onset of expression. Whether time after induction was fifteen minutes, or three hours, inclusion bodies were always present. Similar expression experiments were conducted at lower temperatures, to slow protein synthesis, and to aid in lessening the extent of aggregate formation, but once again, the problem persisted.

Although synthesis of proteins as insoluble inclusion bodies have the advantage in aiding the purification of the protein and protecting it from degradation in the cell (Creighton, 1993), it requires that the protein be solubilized and correctly refolded to yield the active, or native form. Although the addition of a reductant (DTT), metal ions, and glycerol modified refolding conditions, yields of soluble DmpF and DmpG were always low in refolding experiments (Table 2). Dialysis against buffer at pH 7 was chosen for all dialyses, because at this pH the highest yields of soluble protein were obtained (Table 2) and furthermore, DTT is somewhat unstable at high pH. Regardless of the refolding conditions, only DmpF activity was ever reconstituted. Attempts to regenerate the native folded state also were made by concurrently refolding DmpF and DmpG in the same dialysis sac. The rationale behind these refolding experiments was to see if the native enzyme activities could be regenerated when both polypeptides were present. Unfortunately, aldolase activity was not detected, even when the two proteins were co-dialysed. Thus, the inclusion of both proteins during refolding did not help increase the yield of soluble protein molecules, or regenerate aldolase activity.

What all of these experiments seem to indicate is that it is inherently difficult to refold and assemble the DmpFG complex after denaturation. A control unfolding and refolding experiment with pure native enzyme only regenerated 5 % of native aldolase and 7 % native dehydrogenase activity (data not shown). Therefore the denaturation and refolding experiments were inconclusive as to why DmpG always remained inactive. It is possible that under all refolding conditions the protein is misfolded or perhaps it is missing a crucial cofactor, required for proper folding, or the association with its partner, DmpF, is never correct.

After the failure to find conditions under which DmpG could be refolded in an active form, renewed effort was made to achieve overexpression of soluble DmpF and DmpG. The first test was to find out whether DmpF and DmpG could be coexpressed from two separate plasmids in *E. coli*. This did not help either, as inclusion bodies were still formed (data not shown). One possibility could be that these proteins require the aid of a *Pseudomonas* chaperone protein, for proper complex formation, that is missing in *E. coli*. Although this may not be highly probable, because many other *Pseudomonas* proteins have been successfully expressed in *E. coli*, it is still a possibility. Another reason could be that synthesis has to be coordinated by the genes being translated one after the other. This alternative also seems valid, however thus far this claim has not be substantiated by the literature.

Although many of the other *dmp*-operon encoded *meta*- cleavage proteins have been successfully expressed in *E. coli* using the pET expression system both proteins are

foreign to *E. coli*. It was then decided to switch expression of both DmpF and DmpG to *Pseudomonas* PB2701, which may better mimic their native host environment.

Expression of the enzyme in *Pseudomonas* was crucial in obtaining soluble *dmpG*-encoded aldolase. However the *dmpF* - encoded dehydrogenase seemed to form the same relative amount of soluble to insoluble amorphous protein in *Pseudomonas* as in *E. coli*. A 3 L culture of cells was used for purification of the DmpG, using a method essentially the same as that for the native enzyme, with the omission of the ammonium sulfate fractionation step. Surprisingly, the behavior of the DmpG protein, during elution from the DEAE purification column, was essentially the same as that of the native protein. The only major difference observed, aside from gel filtration, was that elution from the hydrophobic phenyl Sepharose column occurred before the end of the gradient, about 40 mL earlier than the native protein under the same conditions (Powlowski, Shingler & Sahlman, 1993). What this seems to suggest is that the protein was less hydrophobic than the native complex. Considering the fact that only 3 L of culture were used, a relatively high amount of protein was recovered (7 mg), and although the ammonium sulphate fractionation step was omitted, the protein was still 95% pure, as judged by SDS-PAGE.

The aldolase protein was inactive after purification, when it was used in two different kinds of aldolase assays (Figure 11). When the same amount of native enzyme was added to similar assays, both reactions would have been finished within one minute. In the case of this purified aldolase, a relatively flat line over 30 minutes in Figure 11 indicates absolutely no catalytic activity. Inactivity of DmpG purified from the

overexpressing *Pseudomonas* strain could result from any one of a number of different factors. Perhaps the active site of the aldolase is in fact shared with the dehydrogenase, or maybe something occurred during the purification procedure to inactivate the protein. It should, however, be noted that the aldolase from the *Pseudomonas* overexpressing strain, never showed any activity throughout the purification procedure. Folding into a soluble misfolded form, or incorrect quaternary structure, are also possible explanations. Thus these experiments did not conclusively demonstrate whether DmpG alone determines aldolase activity or whether the active site is shared with DmpF.

Kinetics data were collected in order to determine the kinetic mechanism of the dehydrogenase. The initial rate plots with acetaldehyde as the varied substance indicate a sequential mechanism. The Km for acetaldehyde appeared to be approximately 50 mM from the Lineweaver-Burk plots (Figure 15). This seems like an extremely high value and is unlikely to be a concentration approached physiologically. In the DmpFG complex, acetaldehyde may normally be channeled from the DmpG to DmpF (see below), so that exogenously added acetaldehyde may not easily find its way to the dehydrogenase active site. This might explain the very high Km for acetaldehyde.

All of the slope and y-intercept replots (Figure 16, Figure 17, Figure 19, Figure 20, and Figure 22) are linear (regression coefficients of 0.993-0.998). Theoretically these lines should be curved towards the origin (Rudolph & Fromm, 1979) but the reason they are not may be because the concentrations of the two constant ratio substrates were kept low to avoid problems such as substrate inhibition, and modification of the native enzyme by

acetaldehyde. Had the concentrations been sufficiently increased to values 20 or 30X Km, curvature may have been observed in the replots.

The sequential mechanism was also confirmed using data collected with NAD^+ as the varied substrate (Figure 18). The apparent Km value for NAD^+ appeared to be approximately 100 μM. One of the plots was considerably off the intersecting point, 120 μM. This value was obtained at the lowest ratio concentrations of acetaldehyde and CoA. When the two lowest concentration points are excluded, the Km becomes 108 μM, which is much closer to the intersection point of 100 μM.

Finally, the initial rate kinetics data using CoA as the varied substrate also indicated a sequential mechanism because all of the plots were again intersecting, but this time on the y-axis (Figure 21). This indicates that the kinetic mechanism involves the formation of a ternary complex of enzyme bound with acetaldehyde, NAD^+, and CoA, before the release of any products. There are two possibilities cited in the literature, consistent with the kinds of primary and replotted data obtained; the equilibrium ordered terreactant system, and the random A/B ordered C binding mechanism (Rudolph & Fromm, 1979).

In the equilibrium ordered terreactant system (Figure 23A), acetaldehyde must bind to the enzyme first, then NAD^+, and finally CoA, in that order, before NADH and acetyl-CoA are released. Alternatively, NAD^+ may bind to the enzyme first, then acetaldehyde and, always finally, CoA. In each of these kinetic mechanisms, the same Lineweaver-Burk patterns would be observed. However it is clear that since all the plots intersect at the

same y-axis when CoA is the varied substrate, (Figure 21), CoA must always be the last substrate to join the ternary complex. Although no examples of an ordered terreactant system have previously been reported, the mechanism appears to be reasonable and is consistent with chemical theory (Fromm & Rudolph, 1979). In general, most dehydrogenases exhibit a preferential binding to NAD^+ first, and then all other substrates (Hempel et al, 1993).

In the random A/B ordered C kinetic mechanism (Figure 23B), acetaldehyde or NAD^+ could randomly bind to free enzyme, but Coenzyme A only binds once the enzyme-NAD^+-acetaldehyde complex is formed. This type of mechanism cannot be distinguished from the ordered terreactant mechanism discussed above, on the basis of the experiments carried out so far. What is interesting is that regardless of which mechanism operates, CoA binds last, and this is consistent with the proposed mechanism of acylating dehydrogenases (Figure 3). Coenzyme A would be the last substrate necessary in order to yield the final product, acetyl-CoA, by thiolysis of the thiohemiacetal intermediate.

In order to distinguish between the two kinetic mechanisms further work using competitive inhibitors might be a possible approach. By using competitive inhibitors in enzyme kinetics experiments it is possible to obtain information about the binding order for many ordered systems (Fromm, 1966). Since the two mechanisms in question have different rate equations, competitive inhibition will yield different double reciprocal plots. An inhibitor for acetaldehyde for the completely ordered system will give an uncompetitive non-linear double reciprocal plot when either NAD^+ or CoA is varied and

competitive inhibition for acetaldehyde (Fromm, 1966). An inhibitor for NAD^+ would show uncompetitive inhibition for acetaldehyde, competitive inhibition vs NAD^+ and non-linear uncompetitive (altered Km and Vmax) inhibition vs CoA (Fromm, 1966). Finally, an inhibitor for CoA will lead to competitive inhibition for CoA, and uncompetitive inhibition vs acetaldehyde and NAD^+ (Fromm, 1966).

On the other hand, in rapid equilibrium random mechanisms, it is assumed that all of the steps in the sequence equilibrate rapidly relative to the interconversion of the quaternary complexes. Thus, while inhibition relative to acetaldehyde would be competitive (altered Km), it would be uncompetitive relative to the other substrates. A similar type of pattern occurs when inhibitors for NAD^+ and CoA are used (Fromm, 1966). Since there are many NAD^+ utilizing enzymes, finding an inhibitor for NAD^+, should not be a difficult task. For instance one reference (Sampathakuna & Morrison, 1982) used AMP and $NADP^+$ for competitive inhibition studies in chorismate mutate prephate dehydrogenase from *E. coli* in order to determine the dehydrogenase's kinetic mechanism. It is also possible to test other nucleotide containing analogues as competitive inhibitors for NAD^+. Since the two types of inhibition patterns that will be observed for the two different mechanisms are completely different, they can be easily distinguished by this method.

The kinetic mechanisms for two other acylating dehydrogenases have been determined as being "ping-pong" mechanisms. Binding of substrates is interrupted by the release of products. Coenzyme A-linked aldehyde dehydrogenase, from *Clostridium kluyveri* undergoes a bi uni uni uni ping-pong mechanism as illustrated in Figure 4 (Smith &

Kaplan, 1980). CoA linked aldehyde dehydrogenase from *E coli*, also undergoes a ping pong reaction sequence similar to the *C. kluyveri* enzyme (Rudolph, Purich & Fromm, 1968). Therefore, the postulated proposed "sequential" mechanisms for the DmpF protein appear to be different from the ping-pong mechanisms already determined in the two aforementioned acylating dehydrogenases.

Having completed the kinetics for the DmpG-coupled dehydrogenase, and direct dehydrogenase assay, the question of substrate channeling could be addressed (Figure 26). Does toxic acetaldehyde channel from one active site to the next in the DmpFG complex, keeping it from diffusing into the cell? Does such a mechanism exist to prevent acetaldehyde from encountering non-acylating aldehyde dehydrogenases, which are less efficient in energetic terms when compared to acylating dehydrogenases such as DmpF?

By comparing the kcat values of the two aldolase coupled reactions (Figure 12), pyruvate to lactate, 108 min^{-1} (detection using lactate dehydrogenase), and acetaldehyde to acetyl CoA, 580 min^{-1} (detection using DmpF), it can be seen that the two maximal velocities are different. What can be interpreted from this difference is that DmpG-produced acetaldehyde is converted into acetyl CoA (by DmpF) almost six times faster than DmpG-produced pyruvate is reduced to lactate by exogeneous LDH. This by itself does not prove that substrate channeling occurs, but it suggests that pyruvate is slow coming off the enzyme. The difference in apparent Km's between the two reactions is reasonable, because the kinetic parameters of the two coupling enzymes are likely to be different. For the aldolase reaction, it should be noted that the presence of the R-isomer of 4-hydroxy-

2-ketovalerate in either aldolase coupled reaction (Figure 13) lowers the Vmax and the Km, which is indicative of an uncompetitive inhibitor.

The question of substrate channeling was investigated by comparing the kinetic parameters of the two individual reactions, starting with acetaldehyde, for assaying dehydrogenase activity, with those for the overall reaction, starting with 4-hydroxy-2-ketovalerate (Figure 26). The overall reaction for the coupled dehydrogenase reaction, 4-hydroxy-2-ketovalerate, to acetaldehyde, to acetyl-CoA, has a kcat of 580 min^{-1}, and that of the direct assay, acetaldehyde to acetyl-CoA, is 54 min^{-1}. There is a tenfold difference between the two maximal velocities, depending on whether acetaldehyde is added exogenously or generated by DmpG from 4-hydroxy-2-ketovalerate. The reaction shown in Figure 26A is far too slow to support the overall reaction (Figure 26B), so acetaldehyde diffusing from the bulk solution into the DmpF active site cannot support the observed turnover rate. Thus substrate channeling seems to be occurring.

The Km of 50 mM for acetaldehyde, measured by providing free acetaldehyde in the assay, is also problematic since it is extremely unlikely that concentrations of acetaldehyde anywhere near this would ever exist physiologically. Instead this result suggests that access of free acetaldehyde to the DmpF active site is severely restricted. Channeling of acetaldehyde from DmpG to DmpF would avoid the accessibility problem.

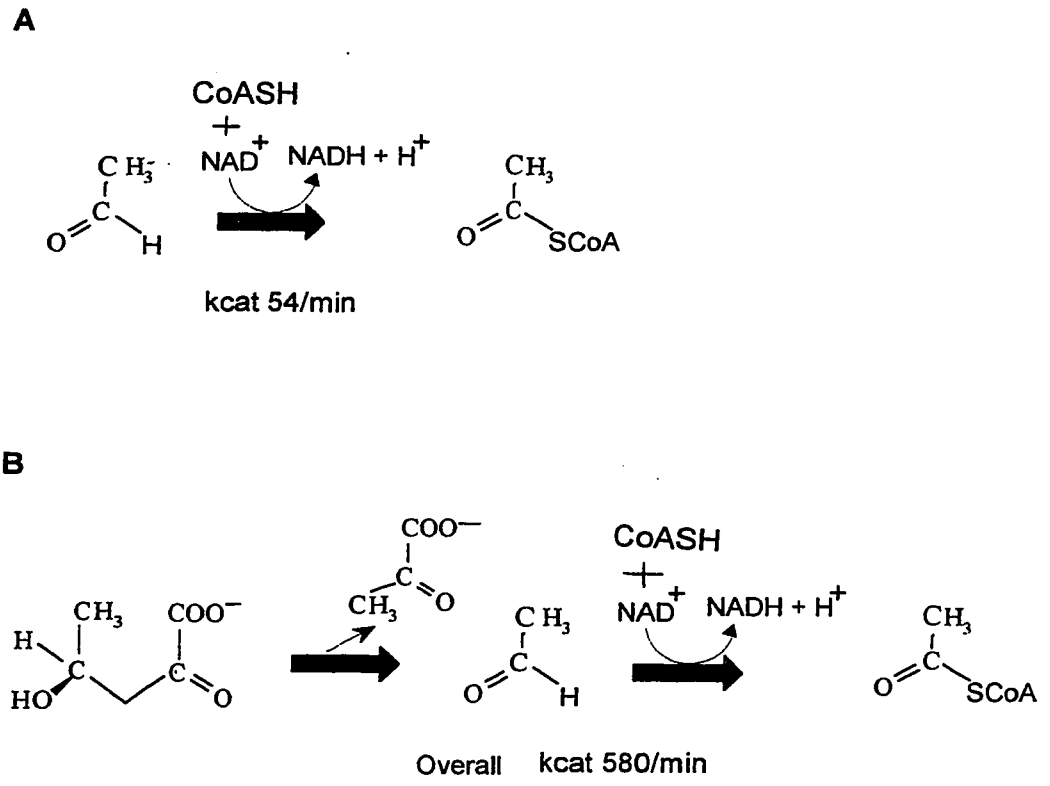

Figure 26: Substrate Channeling in the DmpFG complex. Schematic representation of the two reactions for assaying dehydrogenase activity, as outlined *Materials* and *Methods*.**A:** Represents the standard dehydrogenase reaction, and the *kcat* associated with it. **B:** Represents the ALDH reaction using acetaldehyde generated by DmpG from 4-hydroxy-2-ketovalerate, and its *kcat*.

Some experimental evidence was also collected regarding the modification of active site residues. Modification of native DmpFG by acetaldehyde may result from an accessible positively charged lysine residue, which attacks the carbonyl group of the acetaldehyde. The modification is almost instantaneous, within the first 10 seconds after the initiation of the reaction (Figure 24). At lower concentrations of acetaldehyde, inactivation was also observed when pre-incubating the enzyme with acetaldehyde for several minutes before assaying the dehydrogenase (data not shown). Clearly, more experiments are needed to conclusively determine whether or not the modification is irreversible. However, considering the fact that channeling of acetaldehyde occurs and thus the acetaldehyde levels are unlikely to be very high in the cell, this inhibition is most likely not physiologically relevant.

In order to determine whether one of the two cysteines (Cys 112 and Cys 132) in the dehydrogenase enzyme was involved in dehydrogenase activity, chemical modification of the native enzyme was carried out using a cysteine directed agent, iodoacetate (Figure 25). Iodoacetate works by acetylating and imparting a negative charge on the thiol residue of the cysteine. Dehydrogenase activity was abolished within the first 30 seconds of the reaction whereas aldolase only lost 20% of its overall activity over ten minutes (Figure 25). Considering that at pH 8, iodoacetate is specific for thiols, and that inactivation occurred almost instantaneously under the conditions used, it is reasonable to assume that a cysteine residue crucial for DmpF activity was modified, and that it is the one cysteine residue (Cys 132) that is conserved in the sequence of the dehydrogenase

(Table4). The 20 % loss of activity in aldolase activity after modification with iodoacetate may reflect a conformational change imparted by the iodoacetate after chemical modification of the dehydrogenase. In order to confirm these suggestions site-directed mutagenesis must be successfully carried out.

The creation of a mutant variant will allow the reactions of the aldolase to be examined separately from the dehydrogenase partner. This is inherently interesting because thus far no aldolase activity has been detected in preparations of DmpG. This may be a way of circumventing the problems encountered with inactive preparations obtained from failed independent and coexpressed expression systems.

Bibliography

Bibliography

Anonymous. 1993. Facts and figures for the chemical industry. Chemical Engineering News. **71:** 38-82.

Assinder, S. J., and P. A. Williams. 1990. The TOL plasmids: determinants of the catabolism of toluene and xylenes. Adv. In Microbial Physiology. **31**: 1-69.

Bayly, R. C. and G. J. Wigmore. 1973. Metabolism of phenol and cresols by mutants of *Pseudomonas putida.* Journal of Bacteriology. **113:** 1112-1126.

Bernt, E. and Hans U. Bergenmeyer. 1965. Acetaldehyde determination with alcohol dehydrogenase from yeast. Methods in Enzymatic Analysis. Weinheim/Bergstr. Verlag Chimie. Academic Press. New York.

Brown, R. E., K. L. Jarvis, and K. J. Hyland. 1989. Protein measurement using bicinchoninic acid: elimination of interfering substances. Anal. Biochem. **180:** 136-139.

Burlingame, R., and P. J. Chapman. 1983. Catabolism of phenylpropionic acid and its 3-hydroxy derivative by *Esherichia coli.* Journal of Bacteriology. **155(1):** 113-121.

Chakrabarty, A., M. 1972. Genetic basis of the biodegradation of salicylate in *Pseudomonas*. Journal of Bacteriology. **112**: 815-823.

Clark, D. P., and J. E. Cronan. 1980. Acetaldehyde Coenzyme-A dehydrogenase of *Escherichia coli*. Journal of Bacteriology. **144:** (1) 179-184.

Cleland, W., W. 1963. The kinetics of enzyme-catalyzed reactions with two or more substrates or products. Biochim. Biophys. Acta. **139:** 221-230.

Cooper, S. J., Leonard, G.A., McSweeney, S.M., Thompson, A.W., Naismith, J.H., Qamar, S., Plater, A., Berry, A., and W.N. Hunter. 1996. The crystal structure of a class II fructose-1-6-bisphosphate aldolase shows a novel binuclear metal-binding active site embedded in a familiar fold. Structure. **4(11):** 1303-1315.

Colowick, S. P. and N. O. Kaplan. 1979. Plotting methods for analyzing enzyme rate data. Methods of Enzymology. **63:** 138-159.

Colowick, S. P. and N. O. Kaplan. 1990. Methods in Enzymology Vol 182. Guide to protein purification. Academic Press Inc. New York. Toronto. 264-267.

Cornish-Bowden, A. 1995. Kinetic Consequences of Channeling. A chapter from Channelling in Intermediary Metabolism. Portland Press.

Dagley, S., and D., T., Gibson. 1965. The bacterial degradation of catechol. Biochem. J. **95:** 466-474.

Dagley, S. 1986. Biochemistry of aromatic hydrocarbon degradation in pseudomonads In. Sokatch JR (Ed) The Bacteria. Vol. 10 (pp. 527-556). Academic Press. New York.

Dawson, R., Elliott, D., Elliott, W., and K. Jones. 1986. Data for Biochemical Research, 3rd edition. Clarendon Press. Oxford.

Dreyer, M.K., and G.E. Schulz. 1993. The spatial structure of the class II L-fuculose-1-phosphate aldolase from *E. coli.* Journal of Molecular Biology. **231(3):** 549-533.

Dreyer, M.K., and G.E. Schulz. 1996. Catalytic mechanism of the metal-dependent fuculose aldolase from *Escherichia* coli as derived from the structure. Journal of Molecular Biology. **259(3):** 458-466.

Fromm, H. 1975. Initial Rate Enzyme Kinetics. Springer Verlag. New York. Berlin.

Furukawa, K, et al. 1987. Nucleotide sequence of the 2,3-dihydroxybiphenyl dioxygenases gene of *Pseudomonas pseudoalcaligenes.* Journal of Bacteriology. **169 (1):** 427-429.

Gilberger, T., et al. 1997. Identification and characterization of the functional amino

acids at the active site of the large thioredoxin reductase from *Plasmodium falciparum.* Journal of Biological Chemistry. **272(47):** 29584-29589.

Hanahan, D. 1989. In DNA cloning: A practical approach (Glover, D. M., ed) Vol.1, pp. 109-136, IRL Press Ltd., Oxford.

Harayama, S., Reker, M., Ngai, K. L., and L. N. Ornston. 1989. Physically associated enzymes produce and metabolize 2-hydroxy-2,4-dienoate, a chemically unstable intermediate formed in catechol metabolism via *meta* cleavage in *Pseudomonas putida.* Journal of Bacteriology. **171(11):** 6251-6258.

Harayama, S., and A. Polissi. 1993. In vivo reactivation of catechol 2,3-dioxygenase mediated by a chloroplast type ferredoxin: a bacterial strategy to expand the substrate specificity of aromatic degradative pathways. EMBOJ. **12 (18):** 3339-3347.

Hempel, J., Nicholas, H., and R. Lindahl. 1993. Aldehyde dehydrogenases: Widespread structural and functional diversity within a shared framework. Protein Science. **2:** 1890-1900.

Horecker, B., L., Tsolas, O and C. Y. Lai. 1972. Aldolases. The Enzymes. Third Edition, Volume 7. Academic Press. New York. 213-258.

Kumagai et al. 1970. Tyrosine phenol lyase I. Purification, crystallization, and properties. Journal of Biological Chemistry. **245:** 1767-1777.

Laemmli, U. K. 1970. Cleavage of structural proteins during the assembly of the head of bacteriophage T4. Nature (London). **227:** 680-685.

Lindhahl, R., and J. Hempel. 1990. Aldehyde dehydrogenases: what can be learned from a baker's dozen sequences? Enzymology and Molecular Biology of Carbonyl Metabolism 3. Plenum Press. New York.

Miller, Audrey. 1992. Writing reaction mechanisms in organic chemistry. Academic Press. San Diego, California.

Microsoft® Encarta® 98 Encyclopaedia "Phenol," 1993-1997. © Microsoft Corporation.

Pan, P., Woehl, E., and M. F. Dunn. 1997. Protein architecture, dynamics and allostery in tryptophan synthase channeling. Trends in Biochemical Science. **22(1):** 22-27.

Powlowski, J., Sahlman, L., and V. Shingler. 1993. Purification of the physically associated *meta-* cleavage pathway enzymes 4-hydroxy-2-ketovalerate aldolase and

aldehyde dehydrogenase (acylating) from *Pseudomonas* sp. Strain CF600. Journal of Bacteriology. **175 (2):** 377-385.

Powlowski, J., and Shingler, V. 1994. Genetics and biochemistry of phenol degradation by *Pseudomonas* sp. CF600. Biodegradation. **5:** 219-236.

Powlowski, J., Sealy, J., Shingler, V., and E. Cadieux., 1997. On the role of DmpK, an auxiliary protein associated with multicomponent phenol hydroxylase from *Pseudomonas* sp. Strain CF600. The Journal of Biological Chemistry. **272**: 945-951.

Rudolph, F. B., Purich, D. L., and H. J. Fromm. 1968. Kinetic mechanism of coenzyme-A linked aldehyde dehydrogenase from *E coli.* Journal of Biological Chemistry. **243:** 5539-5545.

Sala-Trepat, J. M., and W. C. Evans. 1971. The metabolic divergence of the *meta* cleavage of catechol by *Pseudomonas putida* NCIB 10015: physiological significance and evolutionary implications. Eur. J. Biochem. **28:** 347-356.

Sambrook, Fritsh, and Maniatis. 1989. Molecular Cloning. Cold Spring Harbour. New York.

Sampathkuman & Morrison. 1982. Chorismate mutase phrephenate dehydrogenase form *E. coli.* Kinetic mechanism of the phrephrenate dehydrogenase reaction.

Biochimica Biophysica Acta. **702:** 212-219.

Segel, I. 1975. Enzyme Kinetics: behaviour and analysis of rapid equilibrium and steady state systems. Wiley. New York. Toronto.

Schagger, H. and G. Von Jagow. 1987. Tricine-sodium dodecyl sulfate-polyacrylamide gel electrophoresis for the separation of proteins in the range from 1 to 100 kDa. Analytical Biochemistry **166**: 368-379.

Schenk, M., Baumann, S., Mattes R. and H. Steinbiss. 1995. Improved high-level expression system for eukaryotic genes in *Escherichia coli* Using T7 RNA Polymerase and Rare Arg-tRNAs. Biotechniques **19:** 196-198

Shingler, V., Franklin, FCH., Tsuda, M., Holroyd, D., and M. Bagdasarian., 1989. Molecular analysis of a plasmid–encoded phenol hydroxylase from *Pseudomonas* sp. Strain CF600. J. Gen. Microbiol. **135**: 1083-1092.

Shingler, V., Powlowski, J., and U. Marklund., 1992. Nucleotide sequence and functional analysis of the complete phenol/ 3,4-dimethylphenol catabolic pathway of *Pseudomonas* sp. strain CF600. Journal of Bacteriology. **174 (3):** 711-724.

Smith,T. L. and N.O. Kaplan. 1980. Purification , properties and kinetic mechanism of coenzyme A-linked aldehyde dehydrogenase from *Clostridium kluyveri.* Archives of Biochemistry and Biophysics. **203 (2): 663-675.**

Spoelestra, S. F. 1977. Degradation of tyrosine in anaerobically stored piggery wastes and pig faeces. Applied Environmental Microbiology. **36:** 631-638.

Sylvestre, M., et al. 1996. 2,3-dihydroxybiphenyl sequencing of *Comamonas testosteroni* strain B-356-biphenylchlorobiphenyl dioxygense genes: evolutionary relationships among Gram-negative bacterial biphenyl dioxygenases. Gene. **174 (2):** 195-202.

Timmis, K. N., Steffan, R. J., and R. Utterman. 1994. Designing microorganisms for the treatment of toxic wastes. Ann. Rev. Microbiol. **48:** 525-557.

Vallee, B. L. and D. Auld. 1992. Functional zinc binding motifs in enzymes and DNA binding proteins. Faraday Discuss. **93:** 43-65.

Wigmore, G. J. and D. Berardino. 1974. *Pseudomonas putida* mutants defective in metabolism of the products of *meta* fission of catechol and its methyl analogues. Journal of Bacteriology. **120:**31-37.